Bioactive exometabolites drive maintenance competition in simple bacterial communities

John L. Chodkowski[1] and Ashley Shade[1,2,3*]

[1]Department of Microbiology and Molecular Genetics, Michigan State University, East Lansing, MI 48824, USA

[2]Department of Plant, Soil and Microbial Sciences, Michigan State University, East Lansing, MI 48824, USA

[3]Program in Ecology, Evolutionary Biology and Behavior, Michigan State University, 10 East Lansing, MI 48824, USA

* Corresponding author and material requests. Email: shadeash@msu.edu; ORCiD: 0000-0002-7189-3067

Competing Interests

The authors declare no competing financial interests.

Abstract

During prolonged resource limitation, bacterial cells can persist in metabolically active states of non-growth. These maintenance periods, such as those experienced in stationary phase, can include upregulation of secondary metabolism and release of exometabolites into the local environment. As resource limitation is common of many environmental microbial habitats, we hypothesized that neighboring bacterial

populations employ exometabolites to compete or cooperate during maintenance, and that these exometabolite-facilitated interactions can drive community outcomes. Here, we evaluated the consequences of exometabolite interactions over stationary phase among three environmental strains: *Burkholderia thailandensis* E264, *Chromobacterium subtsugae*, and *Pseudomonas syringae* pv.*tomato* DC3000. We assembled them into synthetic communities that only permitted chemical interactions. We compared the responses (transcripts) and outputs (exometabolites) of each member with and without neighbors. We found that transcriptional dynamics were changed with different neighbors, and that some of these changes were coordinated between members. The dominant competitor *B. thailandensis* consistently upregulated biosynthetic gene clusters to produce bioactive exometabolites for both exploitative and interference competition. These results demonstrate that competition strategies during maintenance can contribute to community-level outcomes. It also suggests that the traditional concept of defining competitiveness by growth outcomes may be narrow, and that maintenance competition could be an alternative measure.

Introduction

Bacteria interact with other bacteria and their environment within complex, multi-species communities. Bacterial interactions rely on the ability to sense and respond to both biotic and abiotic stimuli [1, 2]. These stimuli include physical, chemical or molecular cues, and can alter bacterial behaviors [3, 4], and ultimately, can also alter community functioning [5, 6]. It is expected that interspecies interactions play an

important role in shaping microbial community dynamics [7]. However, multiple stimuli in the environment make it difficult to disentangle the separate influences of abiotic versus biotic stimuli on microbial community dynamics [8]. Therefore, efforts to characterize and distinguish community responses to biotic stimuli, such as those that facilitate interspecies interactions, will provide insights into the specific roles that microbial interactions play in shaping their communities [9].

Interspecies interactions can be facilitated through small molecules [10]. Extracellular small molecules are collectively referred to as exometabolites [11, 12, 13]. Depending on the exometabolite produced, these molecules can mediate interspecies interactions that range from competitive to cooperative [14]. Of these interaction types, competition has been shown to have a major influence in structuring microbial communities [15, 16, 17]. Thus, competitive interactions that are mediated by exometabolites are also expected to influence to microbial community dynamics. In addition, different types of exometabolites can be employed by bacteria to gain advantage in both exploitative (e.g. nutrient scavenging) and interference (direct cell damage) categories of competition.

Traditionally, competition has been viewed through the lens of resource acquisition [18]. In previous studies, competitiveness is modeled with respect to yield given resource consumption and growth [19, 20]. However, competition for *survival* or *maintenance* may be just as important as competition for yield, especially during periods of resource limitation [21, 22]. Competition during maintenance is likely common in some free-living environments, such as soils, sequencing batch reactors, and the human gut that experience long periods of nutrient famine punctuated by short periods

of nutrient influx [23, 24, 25, 26]. The stationary phase of a bacterial growth curve falls within this context of growth cessation, and pulses of nutrients may be transiently available as cells die and lyse (necromass), while the total population size remains stagnant. Stationary phase is often coordinated with a metabolic shift to secondary metabolism [27, 28]. Therefore, an effective “maintenance” competitor may produce bioactive exometabolites, like antibiotics, which are often produced as a result of secondary metabolism. In particular, bacteria can activate biosynthetic gene clusters (BSGCs) to produce bioactive exometabolites [29]. The activation of BSGCs is closely tied to stress responses, suggesting that bacteria can sense the stress of competition [30, 31]. While it is known that certain exometabolites can trigger BSGC upregulation and, more generally alter transcription [32], there is much to understand about the outcomes of interspecies interactions for BSGCs in multi-member microbial communities.

Here, we build on our previous research to understand how exometabolite-mediated interactions among bacterial neighbors contribute to community outcomes in a simple, three-member community (Table 1). These three members are commonly associated with terrestrial environments (soils or plants) and were chosen because of reported [33] and observed interspecies exometabolite interactions in the laboratory. We used a synthetic community (“SynCom”) approach [34] by applying our previously described transwell system [35], which allowed for evaluation of “community goods” within a media reservoir that was shared among members. The members’ populations were physically isolated by membrane filters at the bottom of each transwell, but could interact chemically via the reservoir. In our prior work, we investigated each member’s

exometabolites and transcription over stationary phase, and the objective was to understand monoculture responses (in minimal glucose media) before assembling the more complex 2- and 3- member communities. We found that each member in monoculture produced a variety of exometabolites in stationary phase, including bioactive molecules involved in competition [36]. In this work, we build to 2- and 3-community memberships to ask: How do members interact via exometabolites in simple communities during maintenance (stationary phase), and what are the competitive strategies and outcomes of those interactions? What genetic pathways, molecules, and members drive the responses? Which outcomes in 3-member community are predicted by the 2-member communities, and which are “greater than the sum of its parts”?

We found that *B. thailandensis* had a major influence on the transcriptional responses of both *C. subtsugae* and *P. syringae*, and that this influence could be attributed to an increase in both interference and exploitative competition strategies. Furthermore, we observed non-additive transcriptional responses and exometabolite production, particularly for *B. thailandensis* with respect to BSGCs. These findings show that diverse competitive strategies can be deployed even when bacterial neighbors are surviving rather than exponentially growing. Therefore, we suggest that contact-independent, exometabolite-mediated interference and exploitation are important competitive strategies in resource-limited environments and support the non-yield outcome of maintenance.

Materials and Methods

112 **Bacterial strains and culture conditions**

113 We selected three environmental bacterial strains for the SynCom experiments
114 that were originally isolated from various plant/soil habitats and that had prior evidence
115 of exometabolite interactions among them in the laboratory [Table 1; 33, 37-40]. Freezer
116 stocks of *B. thailandensis*, *C. subtsugae*, and *P. syringae* were plated on half-
117 concentration Trypticase soy agar (TSA50) at 27°C for at least 24 h. Members were
118 inoculated in 7 ml of M9–0.2% glucose medium and grown for 16 h at 27°C, 200 rpm.
119 Cultures were then diluted into 50 ml M9-0.2% glucose medium such that exponential
120 growth phase was achieved after 10 h of incubation at 27°C, 200 rpm. Members were
121 diluted in 50 ml M9 glucose medium to target ODs (*B. thailandensis* 0.3 OD, *C.*
122 *subtsugae*: 0.035 OD, *P. syringae* 0.035 OD). The high initial OD for *B. thailandensis*
123 was necessary such that stationary phase would be achieved by all members within a 2
124 h window after 24 h incubation in the transwell plate. The glucose concentration in the
125 final dilution varied upon community membership- 0.067% for monocultures, 0.13% for
126 pairwise cocultures, and 0.2% for the 3-member community. For each member, 48 ml of
127 diluted culture was transferred as 4 mL aliquots in 12, 5 mL Falcon tubes to more
128 efficiently prepare replicate transwell plates.

129

130 **Synthetic community experiments**

131

132 Transwell plate preparation was performed as previously described [35]. Briefly,
133 we used sterile filter plates with 0.22-µm-pore polyvinylidene difluoride (PVDF) filter
134 bottoms (Millipore MAGVS2210). Prior to use, filter plates were washed three times with

135 sterile water using a vacuum apparatus (NucleoVac 96 vacuum manifold; Clontech
136 Laboratories). The filter of well H12 was removed with a sterile pipette tip and tweezer,
137 and 31 ml of M9 glucose medium was added to the reservoir through well H12. The
138 glucose concentration in the reservoir varied upon community membership- 0.067% for
139 monocultures, 0.13% for pairwise cocultures, and 0.2% for the 3-member community.
140 Glucose concentration was adjusted to plate occupancy (e.g., 3-member communities
141 had higher number of wells occupied than 2- or 1-member). Our aim was for each
142 member to achieve stationary phase at similar times across all conditions to compare
143 transcripts and exometabolites under similar growth trajectories. In other words,
144 available resources were standardized while keeping the well occupancy for each
145 member constant. With this design, transcripts and exometabolites in cocultures that
146 deviated from those in monocultures could be attributed to interspecies interactions and
147 not complicated by offset in member growth trajectories across the experimental
148 conditions.

149 Each well was filled with 130 µL of culture or medium (prepared as described,
150 above; see methods section: Bacterial strains and culture conditions). For each plate, a
151 custom R script (RandomArray.R [see script at
152 https://github.com/ShadeLab/PAPER_Chodkowski_mSystems_2017/blob/master/R_an
153 alysis/RandomArray.R]) was used to randomize community member placement in the
154 wells so that each member occupied a total of 31 wells per plate. In total, there were 7
155 community conditions- 3 monocultures, 3 pairwise cocultures, and the 3-member
156 community. Each member occupied 31 wells per plate regardless of experimental
157 condition. Thus, “baseline” exometabolites could be determined in the monocultures,

158 and then deviations in exometabolite abundance or detection in the cocultures could be
159 attributed to interspecies interactions. A time course was performed for each replicate.
160 The time course included an exponential phase time point (12.5 h) and 5 time points
161 assessed every 5 h over stationary phase (25 h – 45 h). Four biological replicates were
162 performed for each community condition for a total of 28 experiments. For each
163 experiment, 6 replicate filter plates were prepared for destructive sampling for a total of
164 168 transwell plates.

165 Filter plates were incubated at 27°C with gentle shaking (~0.32 rcf). For each
166 plate, a custom R script (RandomArray.R [see script at
167 https://github.com/ShadeLab/PAPER_Chodkowski_mSystems_2017/blob/master/R_an
168 alysis/RandomArray.R]) was used to randomize wells for each organism assigned to
169 RNA extraction (16 wells) and flow cytometry (5 wells). The following procedure was
170 performed for each organism when a transwell plate was destructively sampled: i) wells
171 containing spent culture assigned to RNA extraction were pooled (~100 µL/well) into a
172 1.7 mL microcentrifuge tube and flash frozen in liquid nitrogen and stored at -80 until
173 further processing. ii) 20 µL from wells assigned for flow cytometry were diluted into 180
174 µL Tris-buffered saline (TBS; 20 mM Tris, 0.8% NaCl [pH 7.4]). In community
175 memberships where *P. syringae* was arrayed with *B. thailandensis*, *P. syringae* had a
176 final dilution of 70-fold in TBS. In community memberships where *P. syringae* was
177 arrayed in monoculture or in coculture with *C. subtsugae*, *P. syringae* had a final dilution
178 of 900-fold in TBS. Final dilutions for *B. thailandensis* and *C. subtsugae* were 1 300-fold
179 and 1 540-fold, respectively. Each member was diluted differently to achieve a suitable
180 events/second range on the flow cytometer for accurate cell counting. Populations were

181 then stained and analyzed on the flow cytometer for live/dead counting (see
182 Supplementary Methods). iii) Spent medium (~31 ml) from the shared reservoir was
183 transferred to 50 mL conical tubes, flash-frozen in liquid nitrogen and stored at −80 °C
184 prior to metabolite extraction.
185

186 **RNA-seq**

187 RNA extraction, sequencing, quality control, and count matrix generation was performed
188 as previously published [36, see Supplementary Methods].
189

190 **Transcriptomics**

191 *Quality filtering and differential gene expression analysis*

192 Count matrices for each member were quality filtered in two steps: genes
193 containing 0 counts in all samples were removed, and genes with a transcript count of
194 ≤10 in more than 90% of samples were removed. DESeq2 [41] was used to extract size
195 factor and dispersion estimates. These estimates were used as external input into
196 ImpulseDE2 for the analysis of differentially regulated genes [42]. ImpulseDE2
197 determines differential expression by comparing longitudinal count datasets. Case-
198 control (Cocultures-monoculture control) analyses were analyzed to identify genes with
199 differences in temporal regulation at an FDR-corrected threshold of 0.01. Genes that
200 passed the FDR threshold were further filtered for genes that had at least one timepoint
201 with a log2 fold-change (LFC) >= 1 or <= -1. Thus, we defined differentially expressed
202 genes (DEGs) as genes that met both the FDR-corrected and LFC thresholds. For each

member, differences in gene regulation between the three coculture conditions was visualized with Venn diagrams using the VennDiagram package [43].

Differentially expressed genes were first determined by comparing each coculture condition to the monoculture control and applying a LFC threshold (see above). We then determined a second set of DEGs by comparing pairwise cocultures to each other. ImpulseDE2 case-control analyses were performed as follows: *B. thailandensis* coculture with *C. subtsugae* (case) compared to *B. thailandensis* coculture with *P. syringae* (control), *C. subtsugae* coculture with *B. thailandensis* (case) compared to *C. subtsugae* coculture with *P. syringae* (control), and *P. syringae* coculture with *B. thailandensis* (case) compared to *P. syringae* coculture with *C, subtsugae* (control). Genes that passed the FDR-corrected threshold of 0.01 based on ImpulseDE2 analysis and had at least one time point with a LFC of >= 1 or <= -1 represented coculture specific DEGs. The DEGs determined from monoculture comparisons and coculture comparisons were then categorically grouped using Clusters of Orthologous Groups (COG).

COG analysis

Protein fasta files were downloaded from NCBI and uploaded to eggNOG-mapper v2 (http://eggnog-mapper.embl.de/) to obtain COGs. The DEGs determined from ImpulseDE2 and LFC thresholds were categorized as upregulated or downregulated based on temporal expression patterns. DEGs with consistent positive LFC throughout all stationary phase time points were categorized as upregulated. DEGs with consistent negative LFC throughout all stationary phase time points were

226 categorized as downregulated. These DEGs were then assigned to COGs, grouped
227 based on temporal up/downregulation patterns, and plotted using ggplot2 [44].
228
229 *Principal coordinates analysis and statistics*
230 We extracted DEGs based on our previously described definition. A variance-
231 stabilizing transformation was performed on normalized gene matrices using the rlog
232 function in DESeq2. A distance matrix based on the Bray-Curtis dissimilarity metric was
233 then calculated on the variance-stabilized gene matrices and principal coordinates
234 analysis was performed using the R package vegan [45]. Principal coordinates were
235 plotted using ggplot2. Coordinates of the first two PCoA axes were used to perform
236 PROTEST analysis using the PROTEST function in vegan. Dissimilarity matrices were
237 used to perform PERMANOVA and variation partitioning and using the adonis and
238 varpart functions in vegan, respectively. The RVAideMemoire package [46] was used to
239 perform a post-hoc pairwise PERMANOVAs.
240
241 *Biosynthetic gene cluster (BSGC) analysis*
242 NCBI accession numbers were uploaded to antiSMASH 6 beta bacterial version
243 [47] to identify genes involved in BSGCs using default parameters. Where possible,
244 literature-based evidence and BSGCs uploaded to MIBiG [48] were used to better
245 inform antiSMASH predictions. Log2 fold-changes (LFCs) were calculated for all
246 predicted biosynthetic genes within each predicted cluster by comparing coculture
247 expression to monoculture expression at each time point. Average LFCs were
248 calculated from all predicted biosynthetic genes within a predicted BSGC at each time

point. Temporal LFC trends were plotted using ggplot2. An upregulated BSGC was defined as a BSGC that had at least two consecutive time points in stationary phase with a LFC > 1.

Network analysis

Unweighted co-expression networks were created from quality filtered and normalized expression data. Networks were generated for pairwise cocultures containing *B. thailandensis*. First, data were quality filtered as previously described (see methods section: *Quality filtering and differential gene expression analysis*). Then, normalized expression data was extracted from DESeq2. Twenty-three and twenty-four RNA-seq samples from each member were used for network analysis in the *B. thailandensis-C. subtsugae and B. thailandensis-P.syringae* cocultures, respectively (24 samples/member; 6 timepoints, 4 biological replicates). Only 23 samples were used in the *B. thailandensis-C. subtsugae* network analysis because RNA-seq failed for *C. subtsugae* at 45 h, biological replicate 2. Interspecies networks were then inferred from the expression data using the context likelihood of relatedness [49] algorithm within the R package Minet [50]. Gene matrices for each coculture pair were concatenated to perform the following analysis. Briefly, the mutual information coefficient was determined for each gene-pair. To ensure robust detection of co-expressed genes, a resampling approach was used as previously described [51]. Then, a Z-score was computed on the mutual information matrix. A Z-score threshold of 4.5 was used to determine an edge in the interspecies network. Interspecies

271 networks were uploaded into Cytoscape version 3.7.1. for visualization, topological
272 analysis, and enrichment analysis [52].

273 Gene annotation and gene ontology (GO) files were obtained for *B.*
274 *thailandensis*, *P. syringae,* and *C. subtsugae* for enrichment analyses. For *B.*
275 *thailandensis,* annotation and ontology files were downloaded from the Burkholderia
276 Genome Database (https://www.burkholderia.com). For *P. syringae*, annotation and
277 ontology files were downloaded from the Pseudomonas Genome Database
278 (http://www.pseudomonas.com/strain/download). Annotation and ontology files for *C.*
279 *subtsugae* were generated using Blast2GO version 5.2.5 [53]. InterProScan [54] with
280 default parameters were used to complement gene annotations from *C. subtsugae*. GO
281 terms were assigned using Blast2GO with default parameters. In addition, genes
282 involved in secondary metabolism were manually curated and added to these files as
283 individual GO terms. These genes were also used to update the GO term GO**:**0017000
284 (antibiotic biosynthetic process), composed of a collection of all the biosynthetic genes.
285 (see methods section: *Biosynthetic gene cluster (BSGC) analysi*s).

286 Topological analysis was performed as follows: Nodes were filtered from each
287 coculture network to only select genes from one member. The GLay community cluster
288 function in Cytoscape was used to determine intra-member modules. Functional
289 enrichment analysis was then performed on the modules using the BiNGO package [55]
290 in Cytoscape.

291 To determine interspecies co-regulation patterns, we filtered network nodes that
292 contained an interspecies edge. Functional enrichment analysis was performed on the
293 collection of genes containing interspecies edges for each member using the BiNGO

294 package in Cytoscape. Genes contained within modules of interest (e.g. modules
295 containing either thailandamide or malleilactone genes) were selected in Cytoscape for
296 visualization. The biosynthetic gene cluster organization of thailandamide and
297 malleilactone were obtained from MIBig and drawn in InkScape.

298 Protein sequences from an interspecies gene of interest (CLV_2968) within a
299 network module that also contained thailandamide genes from the *B. thailandensis-C.*
300 *subtsugae* network and an interspecies gene of interest (PSPTO_1206) within a
301 network module that also contained malleilactone genes from the *B. thailandensis-P.*
302 *syringae* network were obtained. A protein blast for each protein was run against *B.*
303 *thailandensis* protein sequences. *B. thailandensis* locus tags were extracted from the
304 top blast hit from each run. Normalized transcript counts for these 4 genes of interest
305 were plotted in R. Time course gene trajectories were determined using a loess
306 smoothing function.

307

308 *Non-additive gene expression*

309 The quality filtered and normalized expression matrix from each community
310 member was used to extract log2 fold-change (LFC) values within DESeq2. LFCs were
311 calculated by comparing transcript counts from each time point to its respective time
312 point in the monoculture condition. LFCs were converted to fold-changes (FC). Non-
313 additive outcomes were determined based on the null expectation that FCs in the 3-
314 member community should reflect a summation of FCs from the pairwise cocultures.
315 The thresholds for assigning a gene as non-additive upregulation was as follows:

316

317 (TM/MC)/(PWC1/MC+PWC2/MC) >1.5

318

319 Where TM are the gene counts in the 3-member community, MC are the gene counts in
320 the monoculture condition, and PWC1/PWC2 are the gene counts in the pairwise
321 coculture conditions 1 & 2, respectively. We acknowledge that non-additive gene
322 expression can manifest in many ways and that this calculation presents an overly
323 simplified quantification that is intended to begin exploration of the phenomenon. Non-
324 additive gene expression patterns were determined at each time point and plotted using
325 ggplot2. Venn diagrams were also created to analyze the patterns of non-additivity
326 across the time series and between the exponential phase time point and stationary
327 phase times points. Functional enrichment analysis was performed on the collection of
328 genes determined to have non-additive upregulation using the BiNGO package in
329 Cytoscape.

330

331 **Metabolomics**

332 *LCMS, feature detection, and quality control*

333 Standard operating protocols were performed at the Department of Energy Joint
334 Genome Institute as previously described [36]. MZmine2 [56] was used for feature
335 detection and peak area integration as previously described [36]. Select exometabolites
336 were identified in MZmine2 by manual observation of both MS and MS/MS data. We
337 extracted quantities of these identified exometabolites for ANOVA and Tukey HSD post-
338 hoc analysis in R. We filtered features in three steps to identify coculture-accumulated
339 exometabolites. The feature-filtering steps were performed as follows on a per-member

basis: (i) retain features where the maximum peak area abundance occurred in any of the coculture communities ; (ii) a noise filter, the minimum peak area of a feature from a replicate at any time point needed to be 3 times the maximum peak area of the same feature in one of the external control replicates, was applied; (iii) coefficient of variation (CV) values for each feature calculated between replicates at each time point needed to be less than 20% across the time series.

Four final feature data sets from polar and nonpolar analyses in both ionization modes were analyzed in MetaboAnalyst 5.0 [57], as reported in our prior work [36, see Supplementary Methods].

Principal coordinates analysis and statistics

A distance matrix based on the Bray-Curtis dissimilarity metric was used to calculate dissimilarities between exometabolite profiles. Principal coordinates analysis was performed using the R package vegan. Principal coordinates were plotted using ggplot2. Coordinates of the first two PCoA axes were used to perform Protest analysis using the protest function in vegan. Dissimilarity matrices were used to perform PERMANOVA and variation partitioning and using the adonis and varpart functions in vegan, respectively. The RVAideMemoire package was used to perform a post-hoc pairwise PERMANOVAs. Monoculture controls were removed to focus on coculture trends.

Non-additive metabolomics production

We present a simple assessment of additivity and acknowledge that there are other methods and considerations (see *Discussion*). All reference standard normalized, filtered features (across both polarities and ionization modes) were combined. Non-additive outcomes were determined based on the null expectation that fold-changes (FC) in the 3-member community should reflect a summation of FCs from the pairwise cocultures. The thresholds for assigning a metabolomic feature as non-additive production was as follows:

$$(TM)/(PWC1 + PWC2 + PWC3) > 1.5$$

Where TM is the peak area abundance in the 3-member community, and PWC1/PWC2/PWC2 are the peak area abundance in the pairwise coculture conditions 1,2, and 3, respectively. FCs were determined at each time point. A feature was determined to be produced in the 3-member community in a non-additive manner if it was above the FC threshold at least 3 times during stationary phase. At each time point, a Z-scored distribution of FCs was plotted in R. Z-scores were extracted from exometabolite of interest (thailandamide, pyochelin, and capistruin) to plot as vertical ablines on the Z-scored distributions. In addition, the non-additive features were extracted from the dataset to generate a heat map in MetaboAnalyst. Ward's clustering algorithm was used with Euclidean distances from Z-scored data. Data for each sample are the averages from independent time point replicates (n = 2 to 4).

To find statistical support for non-additive exometabolite production in the 3-member community, we created an "expected" time course abundance for identified

385 exometabolites that had non-additive upregulation (thailandamide, pyochelin, and
386 capistruin). The “expected” time course abundance was determined by calculating the
387 summation of peak abundances across pairwise cocultures with *B. thailandensis*. Due
388 to the issue of replicate independence for each time course, the standard deviation
389 would vary depending on what replicates were combined. As a conservative approach,
390 we permuted all possible pairwise coculture combinations and used the replicate
391 combination that resulted in the highest standard deviation. The time course peak
392 abundance of thailandamide, pyochelin, and capistruin from pairwise cocultures with *B.*
393 *thailandensis*, from the 3-member community, and from the “expected” 3-member
394 community were plotted in ggplot2. We then ran a repeated measures permutation
395 ANOVA to compare the time course peak abundance of thailandamide, pyochelin, and
396 capistruin observed in the 3-member community to the “expected” 3-member
397 community. A post-hoc pairwise t-test was performed to observe which time points were
398 statistically significant. We note each iteration of repeated measures ANOVA would
399 result in different statistical result. This was because the replicate identifiers for the
400 “expected” time course were arbitrarily assigned. For this reason, we only considered a
401 test significant if it was consistently below a P threshold of 0.05 across 10 iterations of
402 the code.

403

404 # Results

405 *Overview*

406 Our major data types included both transcriptomics and metabolomics, and we
407 integrate these to interpret SynCom dynamics and interactions. Our longitudinal design
408 resulted in 288 RNAseq samples across the three members, and 168 community
409 metabolomics samples analyzed in each of four mass spectral modes (polar/nonpolar,
410 positive/negative modes = 672 total mass spectral profiles). After quality control, we
411 were left with 281 RNAseq and 605 total mass spectral profiles for the integrated
412 analyses
413 [https://github.com/ShadeLab/Paper_Chodkowski_3member_SynCom_2021/tree/maste
414 r/SummaryOfSamples]. First, we present results of general responses of transcription
415 (section 1) and exometabolomics (section 2), separately. Then, we integrate
416 transcriptomic and metabolomic efforts to determine the upregulation of biosynthetic
417 gene clusters (BSGCs) and identify exometabolites of interest from mass spectrometry
418 (section 3). We then present a transcriptomics co-expression network to ask how the
419 upregulation of BSGCs influenced interspecies interactions through coordinated
420 longitudinal gene expression (section 4). Lastly, we discuss non-additive outcomes in
421 both transcriptional responses and exometabolite output (section 5).

422

423 *1. Stationary phase transcript dynamics of microbial community members*

424 We had four replicate, independent timeseries of each of seven community
425 memberships (three monocultures plus three cocultures of every pair and the 3-member
426 community), and here focus on the coculture analyses to gain insights into community
427 outcomes (Figs. S1 & S2). Differential expressed genes were determined by comparing
428 time series transcript trajectories applying an FDR and LFC threshold (see methods:

429 *Quality filtering and differential gene expression analysis*). First, we compared each
430 coculture to the monoculture control. A range of 153 to 276 genes were differentially
431 expressed by each member in coculture, irrespective of the identity of neighbors (Fig.
432 S3). In addition, each member also had differential gene expression that was unique to
433 a particular neighbor(s). Summarizing across all cocultures, 1089/5639 (19.3%), coding
434 sequences (CDSs), 1991/4393 CDSs (45.3%), and 3274/5576 CDSs (58.7%) DEGs
435 were determined for *B. thailandensis*, *C. subtsugae*, and *P. syringae*, respectively. Both
436 community membership and time contributed to the transcriptional response of each
437 member (Fig. 1, Table S1). Together, these data suggest that there are both general
438 and specific consequences of neighbors for the transcriptional responses of these
439 bacterial community members.

440 Temporal trajectories in transcript profiles were generally reproducible across
441 replicates for each member given a particular community membership (PROTEST
442 analyses, Table S2). Each member had a distinct transcript profile ($0.480 \leq r2 \leq 0.778$
443 by Adonis; P value, 0.001; all pairwise false discovery rate [FDR]-adjusted P values,
444 ≤0.01 except for two community memberships, Table S3). For all ordinations,
445 community membership had the most explanatory value (Axis 1), followed by time (Axis
446 2), with the most variation explained by the interaction between time and membership
447 (Table S1). Membership alone accounted for 60.6% and 77.0% of the variation
448 explained in *C. subtsugae* and *P. syringae* analyses, respectively and 46.3% in the *B.*
449 *thailandensis* analysis (Table S1).

450 When included in the community, *B. thailandensis* strongly determined the
451 transcript profiles of the other two members. For example, the inclusion of *B.*

452 *thailandensis* in a coculture differentiated transcript profiles for both *C. subtsugae* and
453 *P. syringae* (Fig. 1B & 1C). Thus, *B. thailandensis* appears to have had a dominating
454 influence on the transcriptional response of neighbors, and these responses were
455 dynamic with respect to time.

456 We analyzed clusters of orthologous groups of proteins (COGs) to infer the
457 responses of members to their neighbors. Differentially expressed genes were
458 categorized as upregulated or downregulated based on temporal patterns and
459 representation in COGs (Fig. S4). We focused on the largest differences between total
460 DEGs upregulated and total DEGs downregulated within a COG, which provides
461 insights into broad biological processes affected by community membership. COGs with
462 large differences toward upregulation in *B. thailandensis* included cell motility [N],
463 secondary metabolites biosynthesis, transport, and catabolism [Q], and signal
464 transduction mechanisms [T] while COGs with large differences toward downregulation
465 included defense mechanisms [V], energy production and conversion [C], translation,
466 and ribosomal structure and biogenesis [J]. These results suggest that *B. thailandensis*
467 responds to neighbors via downregulation of growth and reproduction and upregulation
468 of secondary metabolism. We therefore hypothesized that *B. thailandensis* was
469 producing bioactive exometabolites against *C. subtsugae* and *P. syringae* to
470 competitively inhibit their growth.

471 Because of the strong transcript response of *C. subtsugae* and *P. syringae* when
472 neighbored with *B. thailandensis* (Fig. 1B & 1C), we focused on COGs within
473 community memberships with *B. thailandensis* (Fig. S4B & S4C, rows 2 & 3). The COG
474 with large differences toward upregulation in both *C. subtsugae* and *P. syringae* were

475 translation, ribosomal structure and biogenesis [J]. COG groups tending toward
476 downregulation in *C. subtsugae* and *P. syringae* were signal transduction mechanisms
477 [T] and secondary metabolites biosynthesis, transport, and catabolism [Q], respectively.
478 These results suggest that the presence of *B. thailandensis* alters its neighbor's ability
479 to respond to the environment and inhibits secondary metabolism.

480 The above analyses focused on DEGs determined by comparing each coculture
481 to the monoculture control. However, we also wanted to understand differences
482 between pairwise-coculture memberships to determine if the alterations in transcripts
483 were attributed to specific memberships (aka interspecies interactions). A total of 436, 1
484 762, and 2 962 DEGs were determined when comparing the *B. thailandensis* pairwise-
485 cocultures, the *C. subtsugae* pairwise-cocultures, and the *P. syringae* pairwise-
486 cocultures, respectively. Categorizing coculture DEGs based COGs and temporal
487 up/downregulation gene trends shows membership-specific effects (Fig. S5). These
488 data suggest coculture-specific transcriptional alterations driven by interspecies
489 interactions. Given the physical separation of members in our SynCom plate system,
490 these interspecies interactions were very likely exometabolite-mediated.

491

492 *2. Stationary phase exometabolite dynamics of microbial communities*

493 Because member populations are physically separated in the SynCom transwell
494 system but allowed to interact chemically, observed transcript responses in different
495 community memberships are inferred to result from exometabolite interactions. Spent
496 medium from the shared medium reservoir was collected from each transwell plate and
497 analyzed using mass spectrometry to detect exometabolites. Our previous manuscript

498 focused on exometabolite dynamics in monocultures [36]. Here, we focused our
499 analysis on those exometabolites that had maximum accumulation in a coculture (either
500 in pairs or in 3-member community). Consistent with the transcript analysis, we found
501 that both community membership and time explained the exometabolite dynamics, and
502 that the explanatory value of membership and time was maintained across all polarities
503 and ionization modes (Fig. 2, Table S4).

504 Temporal trajectories in exometabolite profiles were generally reproducible
505 across replicates with some exceptions (PROTEST analyses, Table S5, Supplementary
506 File 1). Exometabolite profiles were distinct by community membership ($0.475 \leq r2 \leq$
507 0.662 by Adonis; P value, 0.001; all pairwise false discovery rate [FDR]-adjusted P
508 values, ≤ 0.01 except for two comparisons, Table S6), and also dynamic over time. As
509 observed for the member transcript profiles, and the interaction between membership
510 and time had the highest explanatory value for the exometabolite data (Table S4).

511 We found that the *C. subtsugae*-*P. syringae* coculture exometabolite profiles
512 were consistently the most distinct from the other coculture memberships (Fig. 2),
513 supporting, again, that the inclusion of *B. thailandensis* was a major driver of
514 exometabolite dynamics, possibly because it provided the largest or most distinctive
515 contributions to the community exometabolite pool. Indeed, we observed that a majority
516 of the most abundant exometabolites were either detected uniquely in the *B.*
517 *thailandensis* monoculture or accumulated substantially in its included community
518 memberships (Fig. S6). Some exometabolites detected in *B. thailandensis*-inclusive
519 communities were not detected in its monocultures (Fig. S6D), suggesting that the
520 inclusion of neighbors contributed to the accumulation of these particular

521 exometabolites (e.g. upregulation of biosynthetic gene clusters or lysis products). *C.*
522 *subtsugae* and *P. syringae* contributed less to the 3-member community exometabolite
523 profile, as exometabolites detected in the *C. subtsugae-P. syringae* coculture were less
524 abundant and had lower accumulation over time in the 3-member community (Fig.
525 S6A). Together, these results suggest that *B. thailandensis* can suppress or overwhelm
526 expected outputs from neighbors.

527 In summary, we observed both increased accumulation and unique production of
528 exometabolites in pairwise cocultures and in the 3-member community, with *B.*
529 *thailandensis* contributing the most to the shared exometabolite pool as determined by
530 comparisons with its monoculture exometabolite profile. Related, the transcriptional
531 responses of *C. subtsugae* and *P. syringae* in the 3-member community is most similar
532 to their respective transcriptional response when neighbored with *B. thailandensis*
533 alone, despite the presence of the third neighbor.

534

535 *3. B. thailandensis increases competition strategies in the presence of neighbors*

536 We observed relatively unchanged viability in *B. thailandensis* (Fig. S7). On the
537 contrary, we observed a slight reduction (~2.1 log2 fold change) in *C. subtsugae* live cell
538 counts, and a drastic reduction (~4.7 log2 fold change) in *P. syringae* live cell counts,
539 when either member was cocultured with *B. thailandensis* (Figs. S8 & S9; monoculture
540 cell counts vs *B. thailandensis* coculture cells counts). We note that one doubling
541 occurred in *B. thailandensis* and *P. syringae* monocultures, and in *C. violaceum* in
542 pairwise coculture with *P. syringae.* We elaborate on this finding as the possibility of a
543 reductive cell division as described in our previous manuscript [36]. Given this reduction

544 in viability and that there have been competitive interactions between *B. thailandensis*
545 and *C. subtsugae* previously reported [33], we hypothesized that *B thailandensis* was
546 using competition strategies to influence its neighbors via production of bioactive
547 exometabolites. If true, we would expect transcriptional upregulation in *B. thailandensis*
548 biosynthetic gene clusters (BSGC) that encode bioactive exometabolites. Indeed, we
549 found evidence of this when *B. thailandensis* had neighbors (Fig. 3, Table S7). This
550 suggests that *B. thailandensis* responded to neighbors by upregulating genes involved
551 in the production of bioactive compounds, likely to gain a competitive advantage.
552 However, not all BSGCs in *B. thailandensis* were upregulated. Some BSGCs were
553 unaltered or downregulated (Fig. S10). *C. subtsugae* upregulated only 1 BSGC in
554 coculture with *B. thailandensis,* while *P. syringae* did not upregulate any BSGC in any
555 coculture (Figs. S11 & S12). Interestingly, coculturing with *C. subtsugae* and *P.*
556 *syringae* resulted in the upregulation of an unidentified beta-lactone and an unidentified
557 non-ribosomal peptide synthetase (NRPS) in *B. thailandensis*, respectively. Similarly,
558 coculturing with *B. thailandensis* resulted in the upregulation on an unidentified NRPS-
559 Type I polyketide synthase in *C. subtsugae*. We also note that two additional
560 unidentified NRPS passed the LFC threshold of 1 in *C. subtsugae*. However, these
561 were only upregulated at the exponential phase time point and subsequently
562 downregulated or below the LFC threshold in all stationary phase time points.
563 Interspecies interactions led to the upregulation of BSGC in both *B. thailandensis* and
564 *C. subtsugae* and three of these BSGC encode potentially novel bioactive
565 exometabolites.

566 We were able to identify 6 of the 11 exometabolites from the upregulated *B.*
567 *thailandensis* BSGCs and quantify their abundances from mass spectrometry data (Fig.
568 S13, Supplementary File 2). For any given identified exometabolite, it differentially
569 accumulated between community memberships containing *B. thailandensis* (Table S8),
570 particularly when comparing the *B. thailandensis* monoculture compared to each
571 coculture (Table S9). As expected, these identified exometabolites were not detected in
572 community memberships that did not include *B. thailandensis*. Bactobolin was the only
573 identified exometabolite that accumulated in monoculture to equivalent levels of
574 accumulation in all coculture conditions. Thus, *B. thailandensis* increased competition
575 strategies with neighbors through the upregulation and production of many bioactive
576 exometabolites. Of these bioactive exometabolites, three are documented
577 antimicrobials [58, 59, 60], two are siderophores [61, 62], and one is a biosurfactant
578 [63]. We conclude that *B. thailandensis* produced bioactive exometabolites to
579 competitively interact using both interference and exploitative competition strategies
580 [64]. Given that *B. thailandensis* upregulated competition strategies, and responded
581 more broadly in producing competition-supportive exometabolites when grown with
582 neighbors, we hypothesized that these bioactive exometabolites are responsible for the
583 altered transcriptional responses in *C. subtsugae* and *P. syringae*.

584

585 *4. Interspecies co-transcriptional networks reveal coordinated gene expression*
586 *related to competition*

587 We performed interspecies co-expression network analysis to infer interspecies
588 interactions. We used temporal profiles from transcriptional responses to generate co-

589 expression networks for *B. thailandensis-C. subtsugae* and *B. thailandensis-P. syringae*
590 cocultures, respectively (Table S10). As expected, the majority of nodes network had
591 intraspecies edges only, with interspecies edges comprising 1.85% and 1.90% of the
592 total edges in the *B. thailandensis-C. subtsugae* and *B. thailandensis-P. syringae*
593 networks, respectively. We explored interspecies edges for evidence of interspecies
594 transcriptional co-regulation.

595 We performed two analyses (module analysis and GO enrichment) to validate
596 networks and infer interspecies interactions (Fig. S14). Module analysis validated
597 networks as intraspecies modules enriched for biological processes (Supplementary
598 File 3). To infer interspecies interactions, we filtered genes with interspecies edges and
599 performed enrichment analysis (Supplementary File 4). The top enriched Gene
600 Ontology (GO) term for *B. thailandensis* when paired with *C. subtsugae* was antibiotic
601 synthesis of thailandamide, supporting interference competition. Though the top
602 enriched GO term in *B. thailandensis* when paired with *P. syringae* was bacterial-type
603 flagellum-dependent cell motility, antibiotic synthesis of malleilactone was also enriched.
604 Both thailandamide genes from the *B. thailandensis-C. subtsugae* network (Fig. 4) and
605 malleilactone genes from the *B. thailandensis-P. syringae* network (Fig. S15) formed
606 near-complete modules within their respective BSGCs.

607 At least one gene from each of *B. thailandensis's* upregulated BSGCs (Fig. 3)
608 had an interspecies edge, except for rhamnolipid. The top GO term for both *C.*
609 *subtsugae* and *P. syringae* genes that had edges shared *B. thailandensis* was bacterial-
610 type flagellum-dependent motility. Other notable enriched GO processes were efflux
611 activity for *C. subtsugae* and signal transduction for *P. syringae*. Specifically, a DNA

612 starvation/stationary phase gene (CLV04_2968, Fig. 4), *dspA*, was within the network
613 module that also contained thailandamide genes fromthe *B. thailandensis-C. subtsugae*
614 network and a TonB-dependent siderophore receptor gene (PSPTO_1206, Fig. S15)
615 was within the network module that also contained malleilactone genes from the *B.*
616 *thailandensis-P. syringae* network (Supplementary File 5). Interestingly, both
617 CLV04_2968 and PSPTO_1206 were DEGs and downregulated when cocultured with
618 *B. thailandensis* (Figs. S16A & S17A, respectively). Additionally, the closest homolog for
619 *dspA* in *B. thailandensis* was unaltered (BTH_I1284, Supplementary File 6) when
620 cocultured with *C. subtsugae* (Fig. S16B) and the closest homolog to the TonB-
621 dependent receptor in *B. thailandensis* (BTH_I2415, Supplementary File 7) was a DEG
622 and upregulated when cocultured with *P. syrinage* (Fig. S17B). Taken together, these
623 co-expression networks revealed interspecies coordinated expression patterns.

624

625 *5. Distinct member responses when assembled together*

626 Within a complex community, there can be outcomes that are not expected based on
627 interactions that are observed in simpler situations of member pairs [65, 66, 67]. A
628 typical predictive approach uses the additivity assumption, where the null expectation is
629 that a members' outcome in more complex communities is a summation of its outcomes
630 in simpler communities [68]. Patterns that deviate from the assumption arise from
631 biological phenomena that are deemed non-additive. Much emphasis has been placed
632 on predictions on the additive (or non-additive deviation) nature of growth outcomes in
633 more complex environments [15, 69, 70]. Here, we evaluated non-additive
634 transcriptional responses. We identified genes with non-additive upregulation in the 3-

635 member community (Fig. S18, Supplementary File 8, see methods: *Non-additive gene*
636 *expression*). For *B. thailandensis*, most of these genes consistently had nonadditive
637 upregulation throughout stationary phase. Both *P. syringae* and *C. subtsugae* tended to
638 have transient upregulation of genes at a specific timepoint. For each member, there
639 was a stark contrast in genes with non-additivity between the exponential phase
640 timepoint and all stationary phase time points. Notably, the top GO enrichments
641 included antibiotic biosynthesis for *B. thailandensis*, ATPase-coupled sulfate
642 transmembrane transporter activity for *C. subtsugae*, and nickel cation binding for *P.*
643 *syringae* (Supplementary File 9). Of the BSGCs in *B. thailandensis*, multiple genes
644 involved in the production of thailandamide, pyochelin, and capistruin had non-additive
645 upregulation. Since we were able to identify some of these compounds as features
646 within the mass spectral data, we asked if non-additive transcriptional responses
647 corresponded to non-additive exometabolite ouput.

648 Most exometabolite features did not exceed our simple expectations of additivity,
649 as the average fold change across all time points was ~0.6 (Fig. S19). However, we did
650 find that 858 exometabolomic features accumulated in the 3-member community in a
651 non-additive manner (Fig. S20), including thailandamide (Fig. 5) and pyochelin (Fig.
652 S21), but not capistruin (Fig. S22). At the final stationary phase time point (45 h),
653 thailandamide accumulated ~4-fold more and pyochelin accumulated ~3-fold more than
654 the additive expectation. Thailandamide and pyochelin were consistently above 1σ of
655 the average additive fold change for all coculture filtered exometabolites throughout
656 stationary phase (Fig. S19, ablines). We combined peak areas from pairwise cocultures
657 to create an “expected” exometabolite abundance over the time course for

658 thailandamide, pyochelin, and capistruin (Figs. 5, S21, S22, orange). The experimental
659 exometabolite abundance over the time course was significantly different from the
660 "expected" exometabolite abundance for thailandamide, but not for pyochelin and
661 capistruin (repeated measures ANOVA, Table S11). When comparing each time point
662 separately for thailandamide, significance was obtained only for the initial time
663 point(Table S12).

664

665 Discussion

666 Here, we used a synthetic community system to understand how
667 exometabolomic interactions determine members transcriptional responses and
668 exometabolite outputs. Our experiment used a bottom-up approach to compare the
669 seven possible community memberships of three members, and their dynamics in
670 member transcripts and community exometabolites over stationary phase.Differential
671 gene expression across community memberships and over time show that the
672 exometabolites released by a member were sensed and responded to by its neighbors.
673 Furthermore, members' ouputs in monocultures changed because of coculturing, as
674 evidenced by differential exometabolite production. The largest transcriptional
675 alterations in *C. subtsugae* and *P. syringae* occurred when cocultured with *B.*
676 *thailandensis*. Global expression patterns in *C. subtsugae* and *P. syringae* when in the
677 3-member community still resembled expression patterns in pairwise cocultures with *B.*
678 *thailandensis.* These transcriptional alterations in *C. subtsugae* and *P. syringae* were
679 coordinated with increases in *B. thailandensis* competitive strategies (evaluated by

680 BSGC transcript upregulation and exometabolite abundance) . Numerous transcripts
681 and exometabolite were non-additive in the 3-member community, suggesting that
682 predictions of members outcomes in more complex communities will not always be a
683 simple summation of pairwise outcomes. That interactions within a relatively simple
684 community altered the transcriptional responses and exometabolite outputs of each
685 member is important because these kinds of alterations could, in turn, drive changes in
686 community structure and/or function in an environmental setting. For example, it was
687 shown that interspecies interactions more strongly influenced the assembly of *C.*
688 *elegans* gut communities than host-associated factors [71]. Therefore, mechanistic and
689 ecological characterization of interspecies interactions will inform as to the principles
690 that govern emergent properties of microbial communities.

691 Overall, competitive interactions predominated in this synthetic community. Our
692 previous study found that, over stationary phase in monocultures, each member
693 released and accumulated at least one exometabolite documented to be involved in
694 either interference or exploitative competition [36]. This suggests that entry into
695 stationary phase primed members for competitive interactions, whether there were
696 heterospecific neighbors present. We interpret this strategy of preemptive aggression to
697 be especially advantageous to *B. thailandensis,* as it successfully used competitive
698 strategies against both *C. subtsugae* and *P. syringae*. *B. thailandensis's* success was
699 supported by decreased viable *P. syringae* cells when cocultured with *B. thailandensis*.
700 Though *C. subtsugae* viable cell counts were not as affected directly by the coculture
701 with *B. thailandensis*, *B. thailandensis*-produced bactobolin [72] was detected in the
702 shared medium reservoir. Bactobolin is a bacteriostatic antibiotic previously shown to be

703 bioactive against *C. subtsugae* [33] through ribosome binding [58]. But, *C. subtsugae*
704 can resist bactobolin through upregulation of an RND-type efflux pump [73]. This finding
705 also is supported by our data, as all genes coding for the CdeAB-OprM RND-type efflux
706 system were DEGs and upregulated in *C. subtsugae* cocultures with *B. thailandensis*
707 (CLV04_2413-CLV04_2415).

708 When cocultured with *B. thailandensis*, we observed COG groups such as
709 translation, ribosomal structure and biogenesis [J] had large differences toward
710 upregulation in both *C. subtsugae* and *P. syringae*. At first glance, this seems at odds
711 with our interpretation of *B. thailandensis* competitiveness toward *C. subtsugae* and *P.*
712 *syringae*. In other words, how is B. thailandensis effectively competing via interference
713 competition if both *C. subtsugae* and *P. syringae* are upregulating machinery for
714 growth? There is both theoretical [74] and experimental [75] evidence that show how
715 cells treated with antibiotics stimulate ribosomal production to maintain a sufficient
716 number of active ribosomes. As previously mentioned, *B. thailandensis*-produced
717 bactobolin binds to the ribosome and can inhibit *C. subtsugae* [33, 58]. We also have
718 evidence that bactobolin inhibits *P. syringae* (data not shown). It could be that
719 bactobolin is stimulating ribosomal production in *C. subtsugae* and *P. syringae* as a
720 survival mechanism to maintain protein production by maintaining enough active
721 ribosomes.

722 Coculturing can induce secondary metabolism [76, 77, 78] because an
723 exometabolite produced by one microbe can prompt secondary metabolism in a
724 neighbor [31]. We found that coculturing led to the upregulation of numerous BSGCs in
725 *B. thailandensis*. These exometabolites included bactobolin, malleilactone [61, 79;

726 siderophore and cytotoxin], malleobactin [80, 81; siderophore], capistruin [82; lasso
727 peptide], thailandamide [83; polyketide], pyochelin [62; siderophore], rhamnolipids [63;
728 biosurfactants], and two uncharacterized BSGCs encoding nonribosomal peptide
729 synthetases. Of these exometabolites, bactobolin, capistruin, and thailandamide have
730 documented antimicrobial activities through translation inhibition [58], transcription
731 inhibition [59], and inhibition of fatty acid synthesis [60], respectively. For those
732 exometabolites we were able to identify with mass spectrometry, their accumulation in
733 cocultures was correlated with the upregulation of their BSGCs. Furthermore,
734 up/downregulated patterns across all *B. thailandensis* BSGCs is consistent with ScmR
735 global regulatory patterns of secondary metabolism [84]. Though we were not able to
736 pinpoint the exact inducers of BSGCs, exometabolites such as antibiotics [85] and
737 primary metabolites [86] have been documented to induce secondary metabolism in *B.*
738 *thailandensis*. *C. subtsugae* can inhibit *B. thailandensis* [33] but we did not observe *B.*
739 *thailandensis* inhibition based on cell counts. However, we did find that in stationary
740 phase *C. subtsugae*-*B. thailandensis* cocultures, *C. subtsugae* upregulated an
741 uncharacterized hybrid nonribosomal peptide synthetase-type I polyketide synthase. *P.*
742 *syringae* was the least competitive of the three neighbors, as evidenced by a reduction
743 in live cell counts when cocultured with *B. thailandensis*. Also, *P. syringae* did not
744 increase competitive strategies when cocultured, as no BSGCs were upregulated
745 across all coculture conditions. In summary, though all three neighbors had potential to
746 use competitive strategies and maintained competitive strategies in monoculture [36], *B.*
747 *thailandensis* was most successful in cocultures over stationary phase through

748 increased production of exometabolites involved in interference and exploitative
749 competition strategies.

750 Given the upregulation of BSGCs in *B. thailandensis* and the strong
751 transcriptional responses of *C. subtsugae* and *P. syringae* to the presence of *B.*
752 *thailandensis*, we hypothesized that competitive exometabolites were contributing to
753 their community dynamics. Thus, we used a co-expression network analysis with our
754 longitudinal transcriptome series to infer interspecies interactions [87]. This use of this
755 approach was first demonstrated to infer coregulation between a phototroph-heterotroph
756 commensal pair [88]. Our network confirmed that *B. thailandensis* BSGCs had
757 coordinated gene expression patterns with both *C. subtsugae* and *P. syringae*.
758 Interspecies nodes in both networks contained various genes involved in the
759 aforementioned upregulated *B. thailandensis* BSGCs. In particular, we focused on
760 interspecies edges within thailandamide nodes for the *B. thailandensis*-*C. subtsugae*
761 network and interspecies edges within malleilactone nodes for the *B. thailandensis*-*P.*
762 *syringae* network because these were significantly enriched as interspecies nodes. A *C.*
763 *subtsugae* gene of interest, CLV04_2968, was contained within the thailandamide
764 cluster of interspecies nodes. This gene codes for a DNA starvation/stationary phase
765 protection protein and had the highest homology to the Dps protein in *Escherichia coli*
766 across all *C. subtsugae* protein coding genes. Dps mediates tolerance to multiple
767 stressors and *dps* knockouts are more susceptible to thermal, oxidative, antibiotic, iron
768 toxicity, osmotic, and starvation stressors [89]. Interestingly, CLV04_2968 was
769 downregulated when cocultured with *B. thailandensis*, suggesting that *B. thailandensis*
770 attenuates *C. subtsugae* stress tolerance over stationary phase. While we observed a

771 slight decrease in viable *C. subtsugae* cells when cocultured with *B. thailandensis*, one
772 may expect *C. subtsugae* to have increased sensitivity to a subsequent stress [e.g. pH
773 stress; 90] resulting from CLV04_2968 downregulation in the presence of *B.*
774 *thailandensis*.

775 In the *B. thailandensis*-*P. syringae* co-expression network, a *P. syringae* gene of
776 interest, PSPTO_1206, was contained within the malleilactone cluster of interspecies
777 nodes. PSPTO_1206 is annotated as a TonB-dependent siderophore receptor. A *P.*
778 *syringae* iron-acquistion receptor had coordinated expression with a malleilactone,
779 which has been characterized as a siderophore with antimicrobial properties [61].
780 Interestingly, this gene was downregulated when in coculture with *B. thailandensis*. In
781 contrast, the closest TonB-dependent siderophore receptor homolog to PSPTO_1206 in
782 *B. thailandensis*, BTH_I2415, was upregulated in coculture conditions with *P. syringae*.
783 To summarize, co-expression network analysis revealed interspecies coordinated gene
784 expression patterns Though determining directionality was beyond the scope of this
785 analysis, we observed*B. thailandensis*-increased competition strategies were
786 coordinated with a potential decrease in competition strategies in *C. subtsugae* via
787 reduced stress tolerance and in *P. syringae* with reduced iron acquisition ability.

788 A major goal in microbial ecology is to predict community dynamics for purposes
789 of modulating and/or maintaining ecosystem function [91, 92]. At its core, microbial
790 functional properties emerge, in part, from the concerted interactions of multi-species
791 assemblages. Predictions can be complicated by non-additive phenomena that arise in
792 more complex communities. For example, non-additive phenomena have been
793 documented in gene expression [93, 94], growth [69], and fitness [95]. Here, we also

794 have documented non-additive transcriptional responses and exometabolite outputs in
795 our system when combinatorial stimuli were present in the 3-member community. *B.*
796 *thailandensis* BSGCs displayed non-additive phenomena, as we are able show that the
797 transcriptional response of certain BSGCs in the 3-member community was greater
798 than the naive summation of transcriptional response in pairwise memberships.
799 Furthermore, non-additive transcriptional responses resulted in non-additive
800 exometabolite accumulation (e.g. thailandamide & pyochelin) with exceptions (e.g.
801 capistruin). While we realize that our criteria for determining non-additivity was simplistic
802 and arbitrarily defined, we consider the findings from this study to springboard further
803 exploration. Future studies can focus on genes of interest with purposes of modeling
804 transcriptional behaviors [96] to interspecies interactions to investigate non-additive
805 phenomenon. In addition, we only quantified exometabolite accumulation in the shared
806 medium reservoir. Differential release and uptake of bioactive molecules within the
807 community can complicate tracking metabolite dynamics in the system. Thus, analyses
808 that incorporate both intracellular and extracellular metabolomics can provide a more
809 complete understanding of altered microbial metabolism and non-additive exometabolite
810 production under different conditions. Regardless, we documented non-additive
811 accumulation of secondary metabolites involved in both competition strategies. This
812 finding may have implications for high-order interactions, meaning, the nature of the
813 interaction between two members may be altered by the addition of a third member [97].
814 For example, one member could produce sublethal antibiotics in the presence of an
815 antibiotic-sensitive member. The addition of a third member could stimulate the
816 antibiotic producer to increase antibiotic production, altering the nature of the initial

817 interaction from sublethal to lethal for antibiotic-sensitive member [98]. In other words,
818 the nature of interactions may be altered depending on surrounding stimuli that can
819 exacerbate bacterial behaviors not expected by studying the system as simpler parts
820 [66]. Therefore, characterizing transcriptome and metabolome dynamics in microbial
821 communities is expected to inform how non-additive phenomena arise and how they
822 contribute to deviations in predictive models of community outcomes.

823 One feature of our study is that we adjusted glucose concentration depending on
824 plate occupancy. Glucose concentration increased as membership increased, but a
825 member consistently occupied 31 wells across all experimental conditions. One could
826 argue that resource concentration contributed to differences in transcripts and
827 exometabolites and not interspecies interactions. However, DEGs were present when
828 comparing pairwise coculture conditions and these were attributed to differences in
829 temporal regulation of COG categories (Fig. S5). More specifically, regarding BSGCs,
830 an unidentified NRPS was upregulated in *B. thailandensis* when cocultured with *P.*
831 *syringae* but not when cocultured with *C. subtsugae* (Fig. 3) and, an unidentified NRPS-
832 Type I polyketide synthase was upregulated in *C. subtsugae* when cocultured with *B.*
833 *thailandensis* but not when cocultured with *P. syringae* (Fig. S11). These differences
834 occurred in experimental conditions where the glucose concentration was the same.
835 Thus, we are confident that some changes in transcripts and exometabolites are
836 attributable to membership-specific exometabolite-mediated interspecies interactions.
837 As resource concentration and exometabolite output are intertwined, subsequent work
838 could test how initial resources availability determines SynCom outcomes.

839 Our results indicated that each member continued to maintain competitive
840 strategies despite stagnant population growth. *B. thailandensis* upregulated various
841 bioactive exometabolites involved in both interference and exploitative competition
842 when with neighbors. An effective competitor is often defined as by its ability to
843 outcompete neighbors via growth advantage that stems from efficient nutrient uptake
844 and/or biomass conversion rates [99, 100]. We add to this that a competitor can also
845 have a fitness advantage through effective maintenance, which can similarly employ
846 interference or exploitative competitive strategies despite no net growth. Maintenance
847 may ensure survival in some environments that impose a stationary phase lifestyle,
848 where long periods of nutrient depletion are punctuated with short periods of nutrient
849 flux. In these scenarios, it warrants to understand how competitive strategies are
850 deployed in the interim of growth and the extent to which these interactions contribute to
851 long-term community outcomes. Though population levels remain constant, sub-
852 populations of growing cells have been observed in stationary phase [101], and
853 continued production of competitive exometabolites may serve as an advantageous
854 strategy to hinder growth of competitors. In addition, some antibiotics remain effective in
855 non-replicating bacteria [102]. The ability for continued maintenance via effective
856 competition strategies during stationary phase may provide spatiotemporal maintenance
857 of population levels before growth resumption [103]. Alternatively, both growth and non-
858 growth strategies may be occurring simultaneously (e.g. as can occur in biofilms). The
859 heterogeneity of biofilms may provide an environment where a bacterial population
860 contains both stationary cells in the center of the colony with growing cells at the
861 periphery of the colony that compete and alter developmental patterns of neighboring

862 populations [104, 105]. Thus, we expect that insights into the long-term consequences
863 of competition for microbial community outcomes will be gained by considering
864 competition in both active growth and maintenance scenarios.

865

866 **Code availability**

867 Computing code, workflows, and data sets are available at
868 [https://github.com/ShadeLab/Paper_Chodkowski_3member_SynCom_2021]. R
869 packages used during computing analyses included DEseq2 [41], ImpulseDE2 [42],
870 VennDiagram [43], ggplot2 [44], vegan 2.5-4 [45], RVAideMemoire [46], Minet [50],
871 rtracklayer [106], viridis [107], and helper functions [108, 109, 110, 111].

872

873 **Data availability**

874 Genomes for *B. thailandensis*, *C. subtsugae*, and *P. syringae* are available at the
875 National Center for Biotechnology Information (NCBI) under accession
876 numbers NC_007651 (Chromosome I)/NC_007650 (Chromosome
877 II), NZ_PKBZ01000001, and NC_004578 (Chromosome)/NC_004633 (Plasmid
878 A)/NC_004632 (Plasmid B), respectively. An improved annotated draft genome of *C.*
879 *subtsugae* is available under NCBI BioProject accession
880 number PRJNA402426 (GenBank accession number PKBZ00000000). Data for
881 resequencing efforts for *B. thailandensis* and *P. syringae* are under NCBI BioProject
882 accession numbers PRJNA402425 and PRJNA402424, respectively. Metabolomics
883 data and transcriptomics data are also available at the JGI Genome Portal [112] under
884 JGI proposal identifier 502921. MZmine XML parameter files for all analyses can be

viewed at and downloaded from GitHub (see Dataset 7 at https://github.com/ShadeLab/Paper_Chodkowski_MonocultureExometabolites_2020/tree/master/Datasets). Large data files (e.g., MZmine project files) are available upon request. Supplementary files are also available on GitHub (https://github.com/ShadeLab/Paper_Chodkowski_3member_SynCom_2021/tree/master/Supplemental_Files).

Acknowledgements

This material is based upon work supported by the National Science Foundation under grant DEB 1749544 and by Michigan State University. In addition, metabolite analysis and transcript sequencing were provided by a DOE-JGI Community Science Program award (proposal identifier 502921). The work conducted by the U.S. Department of Energy Joint Genome Institute, a DOE Office of Science User Facility, is supported under contract number DE-AC02-05CH11231. J.L.C. was supported by the Eleanor L. Gilmore Fellowship from the Department of Microbiology and Molecular Genetics.

We thank Katherine B. Louie and Benjamin P. Bowen for support in mass spectral analysis.

Competing Interests

The authors declare no competing financial interests.

Author contributions

J.L.C. and A.S. conceived of and designed the study. J.L.C. performed the research and analyses. J.L.C. and A.S. wrote the manuscript.

References

1. Stock, A. M., Robinson, V. L., & Goudreau, P. N. (2000). Two-component signal transduction. Annual Review of Biochemistry, 69, 183–215. https://doi.org/10.1146/annurev.biochem.69.1.183

2. Browning, D. F., & Busby, S. J. W. (2004). The regulation of bacterial transcription initiation. Nature Reviews Microbiology, 2(1), 57–65. https://doi.org/10.1038/nrmicro787

3. Pietschke, C., Treitz, C., Forêt, S., Schultze, A., Künzel, S., Tholey, A., … Fraune, S. (2017). Host modification of a bacterial quorum-sensing signal induces a phenotypic switch in bacterial symbionts. Proceedings of the National Academy of Sciences of the United States of America, 114(40), E8488–E8497. https://doi.org/10.1073/pnas.1706879114

4. Garren, M., Son, K., Tout, J., Seymour, J. R., & Stocker, R. (2016). Temperature-induced behavioral switches in a bacterial coral pathogen. ISME Journal, 10(6), 1363–1372. https://doi.org/10.1038/ismej.2015.216

5. Kato, S., Haruta, S., Cui, Z. J., Ishii, M., & Igarashi, Y. (2005). Stable coexistence of five bacterial strains as a cellulose-degrading community. Applied and Environmental Microbiology, 71(11), 7099–7106. https://doi.org/10.1128/AEM.71.11.7099-7106.2005

6. Megan Steinweg, J., Dukes, J. S., Paul, E. A., & Wallenstein, M. D. (2013). Microbial responses to multi-factor climate change: Effects on soil enzymes. Frontiers in Microbiology, 4, 146. https://doi.org/10.3389/fmicb.2013.00146

7. Aziz, F. A. A., Suzuki, K., Ohtaki, A., Sagegami, K., Hirai, H., Seno, J., … Futamata, H. (2015). Interspecies interactions are an integral determinant of microbial community dynamics. Frontiers in Microbiology, 6, 1148. https://doi.org/10.3389/fmicb.2015.01148

8. Orr, J. A., Vinebrooke, R. D., Jackson, M. C., Kroeker, K. J., Kordas, R. L., Mantyka-Pringle, C., … Piggott, J. J. (2020). Towards a unified study of multiple stressors: Divisions and common goals across research disciplines. Proceedings of the Royal Society B: Biological Sciences, 287(1926), 20200421. https://doi.org/10.1098/rspb.2020.0421

9. Little, A. E. F., Robinson, C. J., Peterson, S. B., Raffa, K. F., & Handelsman, J. (2008). Rules of engagement: Interspecies interactions that regulate microbial communities. Annual Review of Microbiology, 62, 375–401. https://doi.org/10.1146/annurev.micro.030608.101423

10. Phelan, V. V, Liu, W.-T., Pogliano, K., & Dorrestein, P. C. (2011). Microbial metabolic exchange--the chemotype-to-phenotype link. Nature Chemical Biology, 8(1), 26–35. https://doi.org/10.1038/nchembio.739

11. Kell, D. B., Brown, M., Davey, H. M., Dunn, W. B., Spasic, I., & Oliver, S. G. (2005). Metabolic footprinting and systems biology: The medium is the message. Nature Reviews Microbiology, 3(7), 557–565. https://doi.org/10.1038/nrmicro1177

12. Pinu, F. R., & Villas-Boas, S. G. (2017). Extracellular microbial metabolomics: The state of the art. Metabolites, 7(3), 43. https://doi.org/10.3390/metabo7030043

13. Silva, L. P., & Northen, T. R. (2015). Exometabolomics and MSI: Deconstructing how cells interact to transform their small molecule environment. Current Opinion in Biotechnology, 34, 209–216. https://doi.org/10.1016/j.copbio.2015.03.015

14. Großkopf, T., & Soyer, O. S. (2014). Synthetic microbial communities. Current Opinion in Microbiology, 18(1), 72–77. https://doi.org/10.1016/j.mib.2014.02.002

15. Foster, K. R., & Bell, T. (2012). Competition, not cooperation, dominates interactions among culturable microbial species. Current Biology, 22(19), 1845–1850. https://doi.org/10.1016/j.cub.2012.08.005

16. Coyte, K. Z., Schluter, J., & Foster, K. R. (2015). The ecology of the microbiome: Networks, competition, and stability. Science, 350(6261), 663–666. https://doi.org/10.1126/science.aad2602

17. Hibbing, M. E., Fuqua, C., Parsek, M. R., & Peterson, S. B. (2010). Bacterial competition: Surviving and thriving in the microbial jungle. Nature Reviews Microbiology, 8(1), 15–25. https://doi.org/10.1038/nrmicro2259

18. Tilman, D. (1982). Resource Competition and Community Structure. Princeton, NJ, U.S.A.: Princeton University Press.

19. Stewart, F. M., & Levin, B. R. (1973). Partitioning of Resources and the Outcome of Interspecific Competition: A Model and Some General Considerations. The American Naturalist, 107(954), 171–198. https://doi.org/10.1086/282825

20. Smith, H. L. (2011). Bacterial competition in serial transfer culture. Mathematical Biosciences, 229(2), 149–159. https://doi.org/10.1016/j.mbs.2010.12.001

21. Pekkonen, M., Korhonen, J., & Laakso, J. T. (2011). Increased survival during famine improves fitness of bacteria in a pulsed-resource environment. Evolutionary Ecology Research (Vol. 13). Evolutionary Ecology, Ltd.

22. Holt, R. D. (2008). Theoretical perspectives on resource pulses. Ecology, 89(3), 671–681. https://doi.org/10.1890/07-0348.1

23. Schimel, J. P. (2018). Life in dry soils: Effects of drought on soil microbial communities and processes. Annual Review of Ecology, Evolution, and Systematics, 49, 409–432. https://doi.org/10.1146/annurev-ecolsys-110617-062614

24. Chiesa, S. C., Irvine, R. L., & Manning, J. F. (1985). Feast/famine growth environments and activated sludge population selection. Biotechnology and Bioengineering, 27(5), 562–568. https://doi.org/10.1002/bit.260270503

25. Fetissov, S. O. (2017). Role of the gut microbiota in host appetite control: Bacterial growth to animal feeding behaviour. Nature Reviews Endocrinology, 13(1), 11–25. https://doi.org/10.1038/nrendo.2016.150

26. Hiltunen, T., Laakso, J., Kaitala, V., Suomalainen, L. R., & Pekkonen, M. (2008). Temporal variability in detritus resource maintains diversity of bacterial communities. Acta Oecologica, 33(3), 291–299. https://doi.org/10.1016/j.actao.2007.12.002

27. Navarro Llorens, J. M., Tormo, A., & Martínez-García, E. (2010). Stationary phase in gram-negative bacteria. FEMS Microbiology Reviews, 34(4), 476–495. https://doi.org/10.1111/j.1574-6976.2010.00213.x

28. Čihák, M., Kameník, Z., Šmídová, K., Bergman, N., Benada, O., Kofronová, O., … Bobek, J. (2017). Secondary metabolites produced during the germination of Streptomyces coelicolor. Frontiers in Microbiology, 8, 2495. https://doi.org/10.3389/fmicb.2017.02495

29. Medema, M. H., Kottmann, R., Yilmaz, P., Cummings, M., Biggins, J. B., Blin, K., … Glöckner, F. O. (2015). Minimum Information about a Biosynthetic Gene cluster. Nature Chemical Biology, 11(9), 625–631. https://doi.org/10.1038/nchembio.1890

30. Cornforth, D. M., & Foster, K. R. (2013). Competition sensing: The social side of bacterial stress responses. Nature Reviews Microbiology, 11(4), 285–293. https://doi.org/10.1038/nrmicro2977

31. Okada, B. K., & Seyedsayamdost, M. R. (2017). Antibiotic dialogues: Induction of silent biosynthetic gene clusters by exogenous small molecules. FEMS Microbiology Reviews, 41(1), 19–33. https://doi.org/10.1093/femsre/fuw035

32. Goh, E. B., Yim, G., Tsui, W., McClure, J. A., Surette, M. G., & Davies, J. (2002). Transcriptional modulation of bacterial gene expression by subinhibitory concentrations of antibiotics. Proceedings of the National Academy of Sciences of the United States of America, 99(26), 17025–17030. https://doi.org/10.1073/pnas.252607699

33. Chandler, J. R., Heilmann, S., Mittler, J. E., & Greenberg, E. P. (2012). Acyl-homoserine lactone-dependent eavesdropping promotes competition in a laboratory co-culture model. ISME Journal, 6(12), 2219–2228. https://doi.org/10.1038/ismej.2012.69

34. De Roy, K., Marzorati, M., Van den Abbeele, P., Van de Wiele, T., & Boon, N. (2014). Synthetic microbial ecosystems: an exciting tool to understand and apply microbial communities. Environmental Microbiology, 16(6), 1472–1481. https://doi.org/10.1111/1462-2920.12343

35. Chodkowski, J. L., & Shade, A. (2017). A Synthetic Community System for Probing Microbial Interactions Driven by Exometabolites. MSystems, 2(6), e00129-17. https://doi.org/10.1128/msystems.00129-17

36. Chodkowski, J. L., & Shade, A. (2020). Exometabolite Dynamics over Stationary Phase Reveal Strain-Specific Responses. MSystems, 5(6), e00493-20. https://doi.org/10.1128/msystems.00493-20

37. Brett, P. J., DeShazer, D., & Woods, D. E. (1998). Burkholderia thailandensis sp. nov., a Burkholderia pseudomallei-like species. International Journal of Systematic Bacteriology, 48 Pt 1(1), 317–320. https://doi.org/10.1099/00207713-48-1-317

38. Wells, J. S., Trejo, W. H., Principe, P. A., Bush, K., Georgopapadakou, N., Bonner, D. P., & Sykes, R. B. (1982). SQ 26,180, a novel monobactam. I Taxonomy, fermentation and biological properties. The Journal of Antibiotics, 35(2), 184–188. https://doi.org/10.7164/ANTIBIOTICS.35.184

39. Buell, C. R., Joardar, V., Lindeberg, M., Selengut, J., Paulsen, I. T., Gwinn, M. L., … Collmer, A. (2003). The complete genome sequence of the Arabidopsis and tomato pathogen Pseudomonas syringae pv. tomato DC3000. Proceedings of the National Academy of Sciences, 100(18), 10181–10186. https://doi.org/10.1073/PNAS.1731982100

40. Harrison, A. M., & Soby, S. D. (2020). Reclassification of Chromobacterium violaceum ATCC 31532 and its quorum biosensor mutant CV026 to Chromobacterium subtsugae. *AMB Express*, *10*(1), 202. https://doi.org/10.1186/S13568-020-01140-1

41. Love, M. I., Huber, W., & Anders, S. (2014). Moderated estimation of fold change and dispersion for RNA-seq data with DESeq2. Genome Biology, 15, 550. https://doi.org/10.1186/s13059-014-0550-8

42. Fischer, D. S., Theis, F. J., & Yosef, N. (2018). Impulse model-based differential expression analysis of time course sequencing data. Nucleic Acids Research, 46(20), 119. https://doi.org/10.1093/nar/gky675

43. Chen, H. (2018). VennDiagram: Generate High-Resolution Venn and Euler Plots. R package version 1.6.20.

44. Wickham, H. (2016). ggplot2: Elegant Graphics for Data Analysis. Springer-Verlag New York.

45. Oksanen, J., Blanchet, F. G., Friendly, M., Kindt, R., Legendre, P., McGlinn, D., … Wagner, H. (2019). vegan: Community Ecology Package. R package version 2.5-4.

46. Herve M. (2020). RVAideMemoire: testing and plotting procedures for biostatistics. R Packag version 09-77.

47. Blin, K., Shaw, S., Kloosterman, A. M., Charlop-Powers, Z., van Wezel, G. P., Medema, M. H., & Weber, T. (2021). antiSMASH 6.0: improving cluster detection and comparison capabilities. Nucleic Acids Research, 49(W1), W29–W35. https://doi.org/10.1093/NAR/GKAB335

48. Kautsar, S. A., Blin, K., Shaw, S., Navarro-Muñoz, J. C., Terlouw, B. R., van der Hooft, J. J. J., … Medema, M. H. (2020). MIBiG 2.0: a repository for biosynthetic gene clusters of known function. Nucleic Acids Research, 48(D1), D454–D458. https://doi.org/10.1093/NAR/GKZ882

49. Faith, J. J., Hayete, B., Thaden, J. T., Mogno, I., Wierzbowski, J., Cottarel, G., … Gardner, T. S. (2007). Large-scale mapping and validation of Escherichia coli transcriptional regulation from a compendium of expression profiles. PLoS Biology, 5(1), e8. https://doi.org/10.1371/journal.pbio.0050008

50. Meyer, P. E., Lafitte, F., & Bontempi, G. (2008). Minet: A r/bioconductor package for inferring large transcriptional networks using mutual information. BMC Bioinformatics, 9(1), 461. https://doi.org/10.1186/1471-2105-9-461

51. McClure, R. S., Overall, C. C., Mcdermott, J. E., Hill, E. A., Markillie, L. M., Mccue, L. A., … Beliaev, A. S. (2016). Network analysis of transcriptomics expands regulatory landscapes in Synechococcus sp. PCC 7002. Nucleic Acids Research, 44(18), 8810–8825. https://doi.org/10.1093/nar/gkw737

52. Shannon, P., Markiel, A., Ozier, O., Baliga, N. S., Wang, J. T., Ramage, D., … Ideker, T. (2003). Cytoscape: A software Environment for integrated models of biomolecular interaction networks. Genome Research, 13(11), 2498–2504. https://doi.org/10.1101/gr.1239303

53. Götz, S., García-Gómez, J. M., Terol, J., Williams, T. D., Nagaraj, S. H., Nueda, M. J., … Conesa, A. (2008). High-throughput functional annotation and data mining with the Blast2GO suite. Nucleic Acids Research, 36(10), 3420–3435. https://doi.org/10.1093/nar/gkn176

54. Zdobnov, E. M., & Apweiler, R. (2001). InterProScan - An integration platform for the signature-recognition methods in InterPro. Bioinformatics, 17(9), 847–848. https://doi.org/10.1093/bioinformatics/17.9.847

55. Maere, S., Heymans, K., & Kuiper, M. (2005). BiNGO: a Cytoscape plugin to assess overrepresentation of gene ontology categories in biological networks. Bioinformatics (Oxford, England), 21(16), 3448–3449. https://doi.org/10.1093/BIOINFORMATICS/BTI551

56. Pluskal, T., Castillo, S., Villar-Briones, A., & Orešič, M. (2010). MZmine 2: Modular framework for processing, visualizing, and analyzing mass spectrometry-based molecular profile data. BMC Bioinformatics, 11, 395. https://doi.org/10.1186/1471-2105-11-395

57. Pang, Z., Chong, J., Zhou, G., de Lima Morais, D. A., Chang, L., Barrette, M., … Xia, J. (2021). MetaboAnalyst 5.0: narrowing the gap between raw spectra and functional insights. Nucleic Acids Research, (1), gkab382. https://doi.org/10.1093/nar/gkab382

58. Amunts, A., Fiedorczuk, K., Truong, T. T., Chandler, J., Peter Greenberg, E., & Ramakrishnan, V. (2015). Bactobolin A binds to a site on the 70S ribosome distinct from previously seen antibiotics. Journal of Molecular Biology, 427(4), 753–755. https://doi.org/10.1016/j.jmb.2014.12.018

59. Kuznedelov, K., Semenova, E., Knappe, T. A., Mukhamedyarov, D., Srivastava, A., Chatterjee, S., … Severinov, K. (2011). The antibacterial threaded-lasso peptide capistruin inhibits bacterial RNA polymerase. Journal of Molecular Biology, 412(5), 842–848. https://doi.org/10.1016/j.jmb.2011.02.060

60. Wozniak, C. E., Lin, Z., Schmidt, E. W., Hughes, K. T., & Liou, T. G. (2018). Thailandamide, a fatty acid synthesis antibiotic that is coexpressed with a resistant target gene. Antimicrobial Agents and Chemotherapy, 62(9), e00463-18. https://doi.org/10.1128/AAC.00463-18

61. Biggins, J. B., Ternei, M. A., & Brady, S. F. (2012). Malleilactone, a polyketide synthase-derived virulence factor encoded by the cryptic secondary metabolome of Burkholderia pseudomallei group pathogens. Journal of the American Chemical Society, 134(32), 13192–13195. https://doi.org/10.1021/ja3052156

62. Butt, A. T., & Thomas, M. S. (2017). Iron acquisition mechanisms and their role in the virulence of Burkholderia species. Frontiers in Cellular and Infection Microbiology, 7, 460. https://doi.org/10.3389/fcimb.2017.00460

63. Dubeau, D., Déziel, E., Woods, D. E., & Lépine, F. (2009). Burkholderia thailandensis harbors two identical rhl gene clusters responsible for the biosynthesis of rhamnolipids. BMC Microbiology, 9(1), 1–12. https://doi.org/10.1186/1471-2180-9-263

64. Ghoul, M., & Mitri, S. (2016). The Ecology and Evolution of Microbial Competition. Trends in Microbiology, 24(10), 833–845. https://doi.org/10.1016/j.tim.2016.06.011

65. Sanchez-Gorostiaga, A., Bajić, D., Osborne, M. L., Poyatos, J. F., & Sanchez, A. (2019). High-order interactions distort the functional landscape of microbial consortia. PLoS Biology, 17(12), e3000550. https://doi.org/10.1371/journal.pbio.3000550

66. Mickalide, H., & Kuehn, S. (2019). Higher-Order Interaction between Species Inhibits Bacterial Invasion of a Phototroph-Predator Microbial Community. Cell Systems, 9(6), 521-533.e10. https://doi.org/10.1016/j.cels.2019.11.004

67. D'hoe, K., Vet, S., Faust, K., Moens, F., Falony, G., Gonze, D., … Raes, J. (2018). Integrated culturing, modeling and transcriptomics uncovers complex interactions and emergent behavior in a three-species synthetic gut community. ELife, 7, e37090. https://doi.org/10.7554/eLife.37090

68. Momeni, B., Xie, L., & Shou, W. (2017). Lotka-Volterra pairwise modeling fails to capture diverse pairwise microbial interactions. ELife, 6, e25051. https://doi.org/10.7554/eLife.25051.001

69. Pacheco, A. R., Osborne, M. L., & Segrè, D. (2021). Non-additive microbial community responses to environmental complexity. Nature Communications, 12(1), 1–11. https://doi.org/10.1038/s41467-021-22426-3

70. Estrela, S., Sanchez-Gorostiaga, A., Vila, J. C. C., & Sanchez, A. (2021). Nutrient dominance governs the assembly of microbial communities in mixed nutrient environments. ELife, 10, e65948. https://doi.org/10.7554/eLife.65948

71. Ortiz, A., Vega, N. M., Ratzke, C., & Gore, J. (2021). Interspecies bacterial competition regulates community assembly in the C. elegans intestine. ISME J, 1–15. https://doi.org/10.1038/s41396-021-00910-4

72. Duerkop, B. A., Varga, J., Chandler, J. R., Peterson, S. B., Herman, J. P., Churchill, M. E. A., … Greenberg, E. P. (2009). Quorum-sensing control of antibiotic synthesis in Burkholderia thailandensis. Journal of Bacteriology, 191(12), 3909–3918. https://doi.org/10.1128/JB.00200-09

73. Evans, K. C., Benomar, S., Camuy-Vélez, L. A., Nasseri, E. B., Wang, X., Neuenswander, B., & Chandler, J. R. (2018). Quorum-sensing control of antibiotic resistance stabilizes cooperation in Chromobacterium *subtsugae*. ISME J, 12(5), 1263–1272. https://doi.org/10.1038/s41396-018-0047-7

74. Maitra, A., & Dill, K. A. (2016). Modeling the Overproduction of Ribosomes when Antibacterial Drugs Act on Cells. Biophysical Journal, 110(3), 743–748. https://doi.org/10.1016/J.BPJ.2015.12.016

75. Dennis, P. P. (1976). Effects of chloramphenicol on the transcriptional activities of ribosomal RNA and ribosomal protein genes in Escherichia coli. Journal of Molecular Biology, 108(3), 535–546. https://doi.org/10.1016/S0022-2836(76)80135-0

76. Pettit, R. K. (2009). Mixed fermentation for natural product drug discovery. Applied Microbiology and Biotechnology, 83(1), 19–25. https://doi.org/10.1007/s00253-009-1916-9

77. Netzker, T., Fischer, J., Weber, J., Mattern, D. J., König, C. C., Valiante, V., … Brakhage, A. A. (2015). Microbial communication leading to the activation of silent fungal secondary metabolite gene clusters. Frontiers in Microbiology. Frontiers Media S.A. https://doi.org/10.3389/fmicb.2015.00299

78. Zhu, H., Sandiford, S. K., & Van Wezel, G. P. (2014). Triggers and cues that activate antibiotic production by actinomycetes. Journal of Industrial Microbiology and Biotechnology, 41(2), 371–386. https://doi.org/10.1007/s10295-013-1309

79. Truong, T. T., Seyedsayamdost, M., Greenberg, E. P., & Chandler, J. R. (2015). A Burkholderia thailandensis acyl-homoserine lactone-independent orphan LuxR homolog that activates production of the cytotoxin malleilactone. Journal of Bacteriology, 197(21), 3456–3462. https://doi.org/10.1128/JB.00425-15

80. Alice, A. F., López, C. S., Lowe, C. A., Ledesma, M. A., & Crosa, J. H. (2006). Genetic and transcriptional analysis of the siderophore malleobactin biosynthesis and transport genes in the human pathogen Burkholderia pseudomallei K96243. Journal of Bacteriology, 188(4), 1551–1566. https://doi.org/10.1128/JB.188.4.1551-1566.2006

81. Gupta, A., Bedre, R., Thapa, S. S., Sabrin, A., Wang, G., Dassanayake, M., & Grove, A. (2017). Global Awakening of Cryptic Biosynthetic Gene Clusters in Burkholderia thailandensis. ACS Chemical Biology, 12(12), 3012–3021. https://doi.org/10.1021/acschembio.7b00681

82. Knappe, T. A., Linne, U., Zirah, S., Rebuffat, S., Xie, X., & Marahiel, M. A. (2008). Isolation and structural characterization of capistruin, a lasso peptide predicted from the genome sequence of Burkholderia thailandensis E264. Journal of the American Chemical Society, 130(34), 11446–11454. https://doi.org/10.1021/ja802966g

83. Ishida, K., Lincke, T., Behnken, S., & Hertweck, C. (2010). Induced biosynthesis of cryptic polyketide metabolites in a Burkholderia thailandensis quorum sensing mutant. Journal of the American Chemical Society, 132(40), 13966–13968. https://doi.org/10.1021/ja105003g

84. Mao, D., Bushin, L. B., Moon, K., Wu, Y., & Seyedsayamdost, M. R. (2017). Discovery of scmR as a global regulator of secondary metabolism and virulence in Burkholderia thailandensis E264. Proceedings of the National Academy of Sciences of the United States of America, 114(14), E2920–E2928. https://doi.org/10.1073/pnas.1619529114

85. Okada, B. K., Wu, Y., Mao, D., Bushin, L. B., & Seyedsayamdost, M. R. (2016). Mapping the Trimethoprim-Induced Secondary Metabolome of Burkholderia thailandensis. ACS Chemical Biology, 11(8), 2124–2130. https://doi.org/10.1021/acschembio.6b00447

86. Li, A., Mao, D., Yoshimura, A., Rosen, P. C., Martin, W. L., Gallant, É., … Seyedsayamdost, M. R. (2020). Multi-omic analyses provide links between low-dose antibiotic treatment and induction of secondary metabolism in Burkholderia thailandensis. MBio, 11(1), e03210-19. https://doi.org/10.1128/mBio.03210-19

87. McClure, R. S. (2019). Toward a Better Understanding of Species Interactions through Network Biology. MSystems, 4(3), e00114-19. https://doi.org/10.1128/msystems.00114-19

88. McClure, R. S., Overall, C. C., Hill, E. A., Song, H.-S., Charania, M., Bernstein, H. C., … Beliaev, A. S. (2018). Species-specific transcriptomic network inference of interspecies interactions. ISME J, 12(8), 2011–2023. https://doi.org/10.1038/s41396-018-0145-6

89. Karas, V. O., Westerlaken, I., & Meyer, A. S. (2015). The DNA-binding protein from starved cells (Dps) utilizes dual functions to defend cells against multiple stresses. Journal of Bacteriology, 197(19), 3206–3215. https://doi.org/10.1128/JB.00475-15

90. Nair, S., & Finkel, S. E. (2004). Dps protects cells against multiple stresses during stationary phase. Journal of Bacteriology, 186(13), 4192–4198. https://doi.org/10.1128/JB.186.13.4192-4198.2004

91. Antwis, R. E., Griffiths, S. M., Harrison, X. A., Aranega-Bou, P., Arce, A., Bettridge, A. S., … Sutherland, W. J. (2017). Fifty important research questions in microbial ecology. FEMS Microbiology Ecology, 93(5), fix044. https://doi.org/10.1093/femsec/fix044

92. Konopka, A. (2009). What is microbial community ecology. ISME J, 3(11), 1223–1230. https://doi.org/10.1038/ismej.2009.88

93. Cornforth, D. M., Popat, R., McNally, L., Gurney, J., Scott-Phillips, T. C., Ivens, A., … Brown, S. P. (2014). Combinatorial quorum sensing allows bacteria to resolve their social and physical environment. Proceedings of the National Academy of Sciences of the United States of America, 111(11), 4280–4284. https://doi.org/10.1073/pnas.1319175111

94. Bundy, B. M., Collier, L. S., Hoover, T. R., & Neidle, E. L. (2002). Synergistic transcriptional activation by one regulatory protein in response to two metabolites. Proceedings of the National Academy of Sciences of the United States of America, 99(11), 7693–7698. https://doi.org/10.1073/pnas.102605799

95. Morin, M., Pierce, E. C., & Dutton, R. J. (2018). Changes in the genetic requirements for microbial interactions with increasing community complexity. ELife, 7, e37072. https://doi.org/10.7554/eLife.37072

96. Dukler, N., Gulko, B., Huang, Y. F., & Siepel, A. (2016). Is a super-enhancer greater than the sum of its parts? Nature Genetics, 49(1), 2. https://doi.org/10.1038/NG.3759

97. Billick, I., & Case, T. J. (1994). Higher order interactions in ecological communities: What are they and how can they be detected? Ecology, 75(6), 1529–1543. https://doi.org/10.2307/1939614

98. Bernier, S. P., & Surette, M. G. (2013). Concentration-dependent activity of antibiotics in natural environments. Frontiers in Microbiology, 4, 20. https://doi.org/10.3389/fmicb.2013.00020

99. Miller, T. E., Burns, J. H., Munguia, P., Walters, E. L., Kneitel, J. M., Richards, P. M., … Buckley, H. L. (2005). A critical review of twenty years' use of the resource-ratio theory. American Naturalist, 165(4), 439–448. https://doi.org/10.1086/428681

100. De Jong, H., Casagranda, S., Giordano, N., Cinquemani, E., Ropers, D., Geiselmann, J., & Gouzé, J. L. (2017). Mathematical modelling of microbes: Metabolism, gene expression and growth. Journal of the Royal Society Interface, 14(136), 20170502. https://doi.org/10.1098/rsif.2017.0502

101. Jõers, A., Liske, E., & Tenson, T. (2020). Dividing subpopulation of Escherichia coli in stationary phase. Research in Microbiology, 171(3–4), 153–157. https://doi.org/10.1016/j.resmic.2020.02.002

102. McCall, I. C., Shah, N., Govindan, A., Baquero, F., & Levin, B. R. (2019). Antibiotic killing of diversely generated populations of nonreplicating bacteria. Antimicrobial Agents and Chemotherapy, 63(7), e02360-18. https://doi.org/10.1128/AAC.02360-18

103. Chesson, P. L. (1983). Coexistence of Competitors in a Stochastic Environment: The Storage Effect. Lecture Notes in Biomathematics, 52, 188–198. https://doi.org/10.1007/978-3-642-87893-0_25

104. Stewart, P. S., & Franklin, M. J. (2008). Physiological heterogeneity in biofilms. Nature Reviews Microbiology 2008 6:3, 6(3), 199–210. https://doi.org/10.1038/nrmicro1838

105. Traxler, M. F., Seyedsayamdost, M. R., Clardy, J., & Kolter, R. (2012). Interspecies modulation of bacterial development through iron competition and siderophore piracy. Molecular Microbiology, 86(3), 628. https://doi.org/10.1111/MMI.12008

106. Lawrence, M., Gentleman, R., & Carey, V. (2009). rtracklayer: An R package for interfacing with genome browsers. Bioinformatics, 25(14), 1841–1842. https://doi.org/10.1093/bioinformatics/btp328

107. Garnier, S., Ross, N., Rudis, R., Camargo, P. A., Sciaini, M., & Scherer, C. (2021). viridis - Colorblind-Friendly Color Maps for R, R package, https://sjmgarnier.github.io/viridis/. https://doi.org/10.5281/zenodo.4679424

108. Wickham, H. (2007). Reshaping data with the reshape package. Journal of Statistical Software, 21(12), 1–20. https://doi.org/10.18637/jss.v021.i12

109. Wickham, H. (2019). stringr: Simple, Consistent Wrappers for Common String Operations. R package version 1.4.0.

110. Wickham, H., Averick, M., Bryan, J., Chang, W., McGowan, L., François, R., … Yutani, H. (2019). Welcome to the Tidyverse. Journal of Open Source Software, 4(43), 1686. https://doi.org/10.21105/joss.01686

111. Wickham, H., François, R., Henry, L., & Müller, K. (2019). dplyr: A Grammar of Data Manipulation. R package version 0.8.3.

112. Nordberg, H., Cantor, M., Dusheyko, S., Hua, S., Poliakov, A., Shabalov, I., … Dubchak, I. (2014). The genome portal of the Department of Energy Joint Genome Institute: 2014 updates. Nucleic Acids Research, 42, D26-31. https://doi.org/10.1093/nar/gkt1069

Figure and Table captions

Figure 1. Transcriptional responses are driven by community membership and time. Shown are principal coordinates analysis (PCoA) plots for *B. thailandensis* (Bt, A), *C. subtsugae* (Cs, B), and *P. syringae* (Ps, C). Each point represents a mean transcript

1363 profile for a community member given a particular community membership (neighbor(s)
1364 included, indicated by symbol color) and sampled at a given time point over exponential
1365 and stationary phases (in hours since inoculation, h, indicated by symbol size, n=3 to 4
1366 replicates per timepoint/community membership). The Bray-Curtis distance metric was
1367 used to calculate dissimilarities between transcript profiles. Error bars are 1 standard
1368 deviation around the mean axis scores.
1369

1370 **Figure 2. Bacterial community exometabolite profiles differ by community**
1371 **membership and time.** Shown are PCoA plots for exometabolite profiles from the
1372 following mass spectrometry modes: polar positive (A), polar negative (B), nonpolar
1373 positive (C), and nonpolar negative (D). Each point represents the mean exometabolite
1374 profile (relative contributions by peak area) given a particular community membership
1375 (indicated by symbol color) at a particular time point (indicated by symbol shape). The
1376 Bray-Curtis distance metric was used to calculate dissimilarities between exometabolite
1377 profiles. Error bars are 1 standard deviation around the mean axis scores (n= 2 to 4
1378 replicates). Bt is *B. thailandensis*, Cs is *C. subtsugae*, and Ps is *P. syringae*.
1379

1380 **Figure 3. *B. thailandensis* upregulates biosynthetic gene clusters (BSGC) in**
1381 **cocultures.** Columns represent community membership where Bt: *B. thailandensis*, Cs:
1382 *C. subtsugae*, and Ps: *P. syringae* and rows represent BSCC in *B. thailandensis*. Genes
1383 part of a BSGC were curated from antiSMASH predictions and literature-based
1384 evidence. Within each BSGC, log2 fold-changes (LFC) were calculated by comparing
1385 gene counts from a coculture to the monoculture control at each time point. LFC were

1386 then averaged from all biosynthetic genes in the BSGC at each time point. We defined
1387 an upregulated BSGC as a BSGC that had at least two consecutive stationary phase
1388 time points with a LFC > 1 (indicated by the horizontal line). Note that plots for each
1389 BSGC have separate scales for the Y-axis.
1390
1391 **Figure 4. *B. thailandensis* genes involved in thailandamide production are**
1392 **detected as interspecies edges in the *B. thailandensis*-*C. subtsugae* co-**
1393 **expression network and biosynthetic genes organize into network modules.** A
1394 network module containing the thailandamide BSGC is shown. The network module
1395 nodes are color coded by *B. thailandensis* gene type (BSGC or not) and type of
1396 connections (interspecies or not): thailandamide biosynthetic genes that had
1397 interspecies edges (magenta), thailandamide biosynthetic genes that did not have
1398 interspecies edges (orange), or other genes that were not part of the BSGC (yellow); as
1399 well as genes that were from *C. subtsugae* (blue). The chromosomal organization of the
1400 thailandamide BSGC is shown below the network module. The same colors are applied
1401 to the BSGC operon. The operons also depict genes that were not detected within the
1402 interspecies network, shown in gray. Asterisks indicate core biosynthetic genes in the
1403 BSGCs, as predicted from antiSMASH. The table shows upregulated *B. thailandensis*
1404 BSGCs (Fig. 3) and whether there were interspecies edges detected (check is yes, x is
1405 no).
1406
1407 **Figure 5. Thailandamide accumulates in a non-additive manner.** The accumulation
1408 of thailandamide was quantified through time (n = 3-4 integrated peak areas per time

point). The bottom and top of the box are the first and third quartiles, respectively, and the line inside the box is the median. The whiskers extend from their respective hinges to the largest value (top), and smallest value (bottom) was no further away than 1.5× the interquartile range. Colors correspond to the community membership for the B.thailandensis-P. syringae coculture (yellow, BtPs), the B. thailandensis-C, subtsugae coculture (magenta, BtCs), the “expected” exometabolite abundance in the 3-member community obtained from additive peak areas from the B.thailandensis-P. syringae and B.thailandensis-C, subtsugae cocultures (orange, BtCs+BtPs), and the 3-member community (black, BtCsPs).

Table 1. Bacterial members used in the synthetic community (SynCom) system.

Figure 1

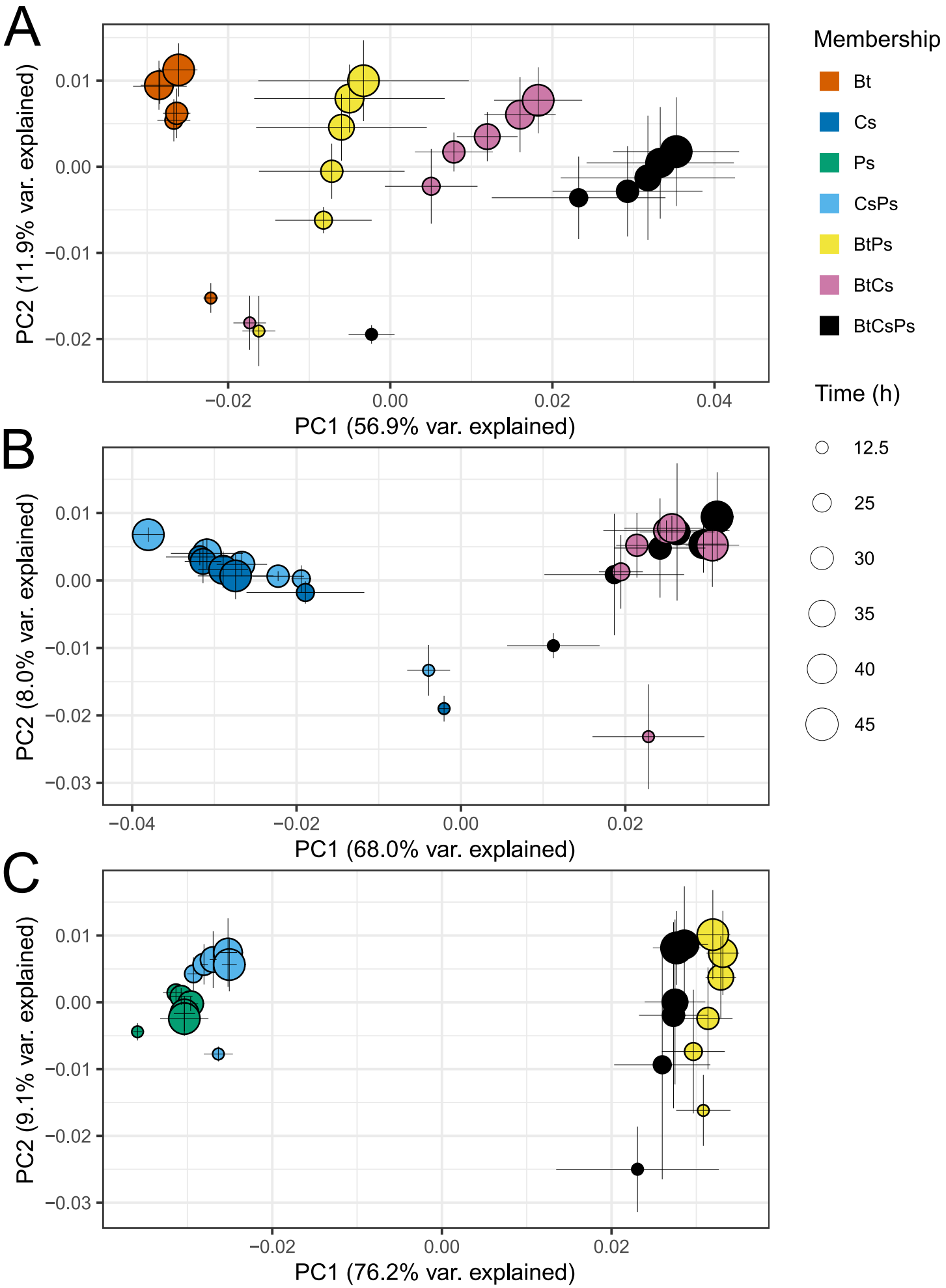
A
PC2 (11.9% var. explained)
PC1 (56.9% var. explained)
0.01
0.00
−0.01
−0.02
−0.02
0.00
0.02
0.04
B
PC2 (8.0% var. explained)
PC1 (68.0% var. explained)
0.01
0.00
−0.01
−0.02
−0.03
−0.04
−0.02
0.00
0.02
C
PC2 (9.1% var. explained)
PC1 (76.2% var. explained)
0.01
0.00
−0.01
−0.02
−0.03
−0.02
0.00
0.02
Membership
Bt
Cs
Ps
CsPs
BtPs
BtCs
BtCsPs
Time (h)
12.5
25
30
35
40
45

Figure 2

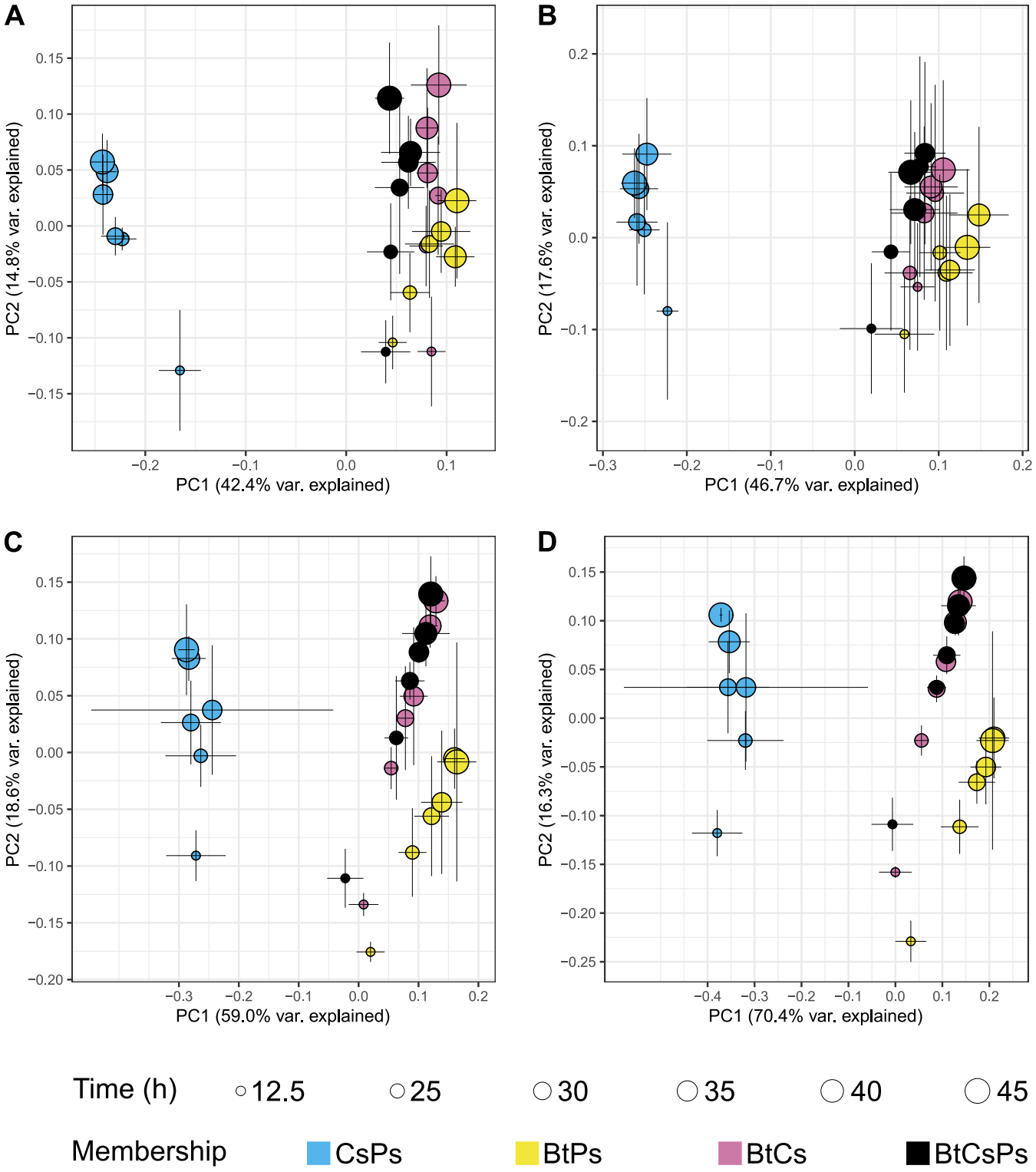
A
PC2 (14.8% var. explained)
PC1 (42.4% var. explained)
B
PC2 (17.6% var. explained)
PC1 (46.7% var. explained)
C
PC2 (18.6% var. explained)
PC1 (59.0% var. explained)
D
PC2 (16.3% var. explained)
PC1 (70.4% var. explained)
Time (h)
12.5
25
30
35
40
45
Membership
CsPs
BtPs
BtCs
BtCsPs

Figure 3

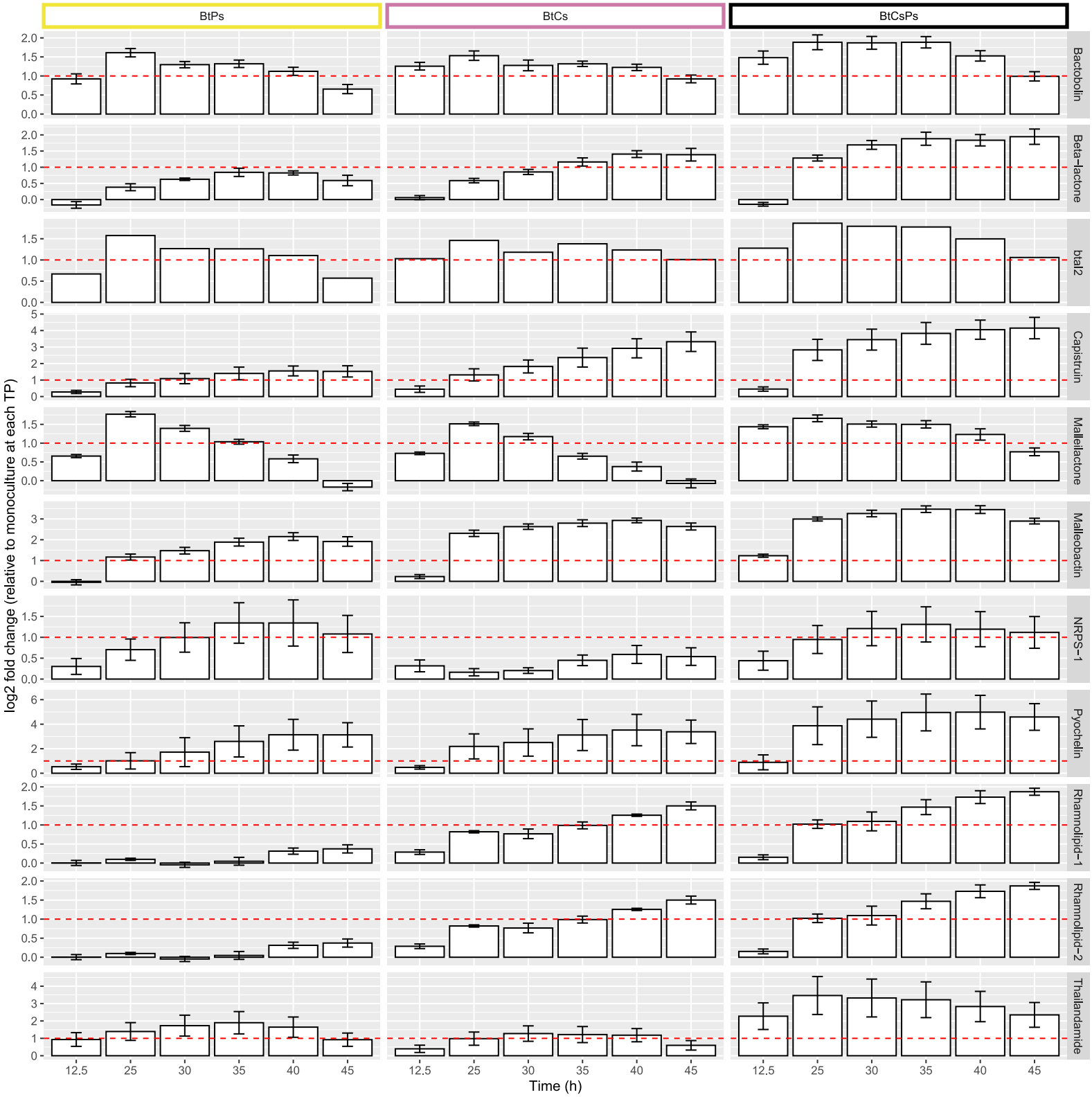
BtPs
BtCs
BtCsPs
Bactobolin
Beta−lactone
btal2
Capistruin
Malleilactone
Malleobactin
NRPS−1
Pyochelin
Rhamnolipid−1
Rhamnolipid−2
Thailandamide
log2 fold change (relative to monoculture at each TP)
Time (h)
12.5
25
30
35
40
45

Figure 4

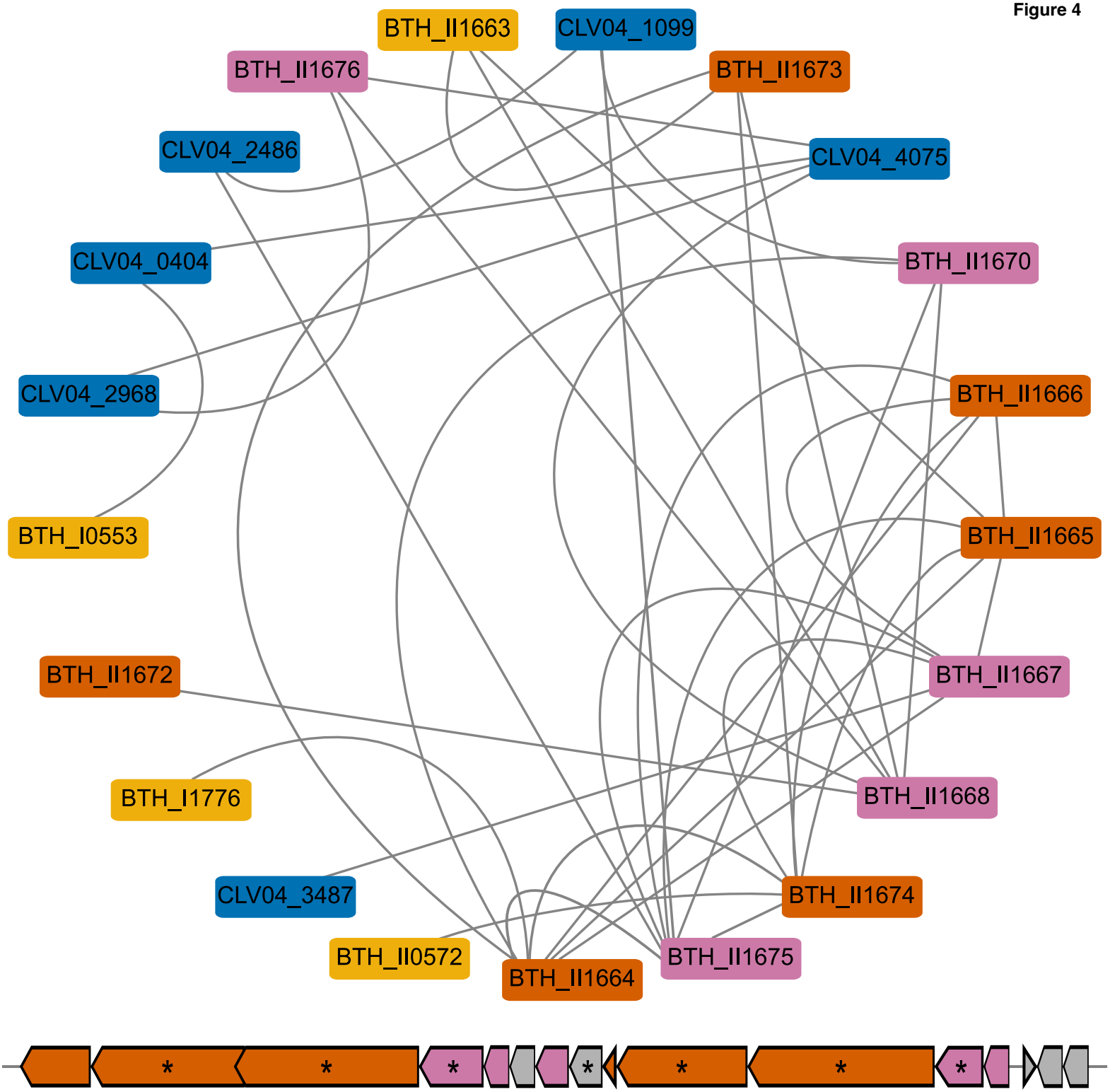

	B. thailandensis-C. subtsugae interspecies network	*B. thailandensis-P. syringae* interspecies network
Bactobolin	✓	✓
Beta-lactone	✓	×
Capistruin	✓	✓
Malleilactone	✓	✓
Malleobactin	✓	✓
NRPS-1	×	✓
Pyochelin	✓	✓
Rhamnolipid	×	×
Thailandamide	✓	✓

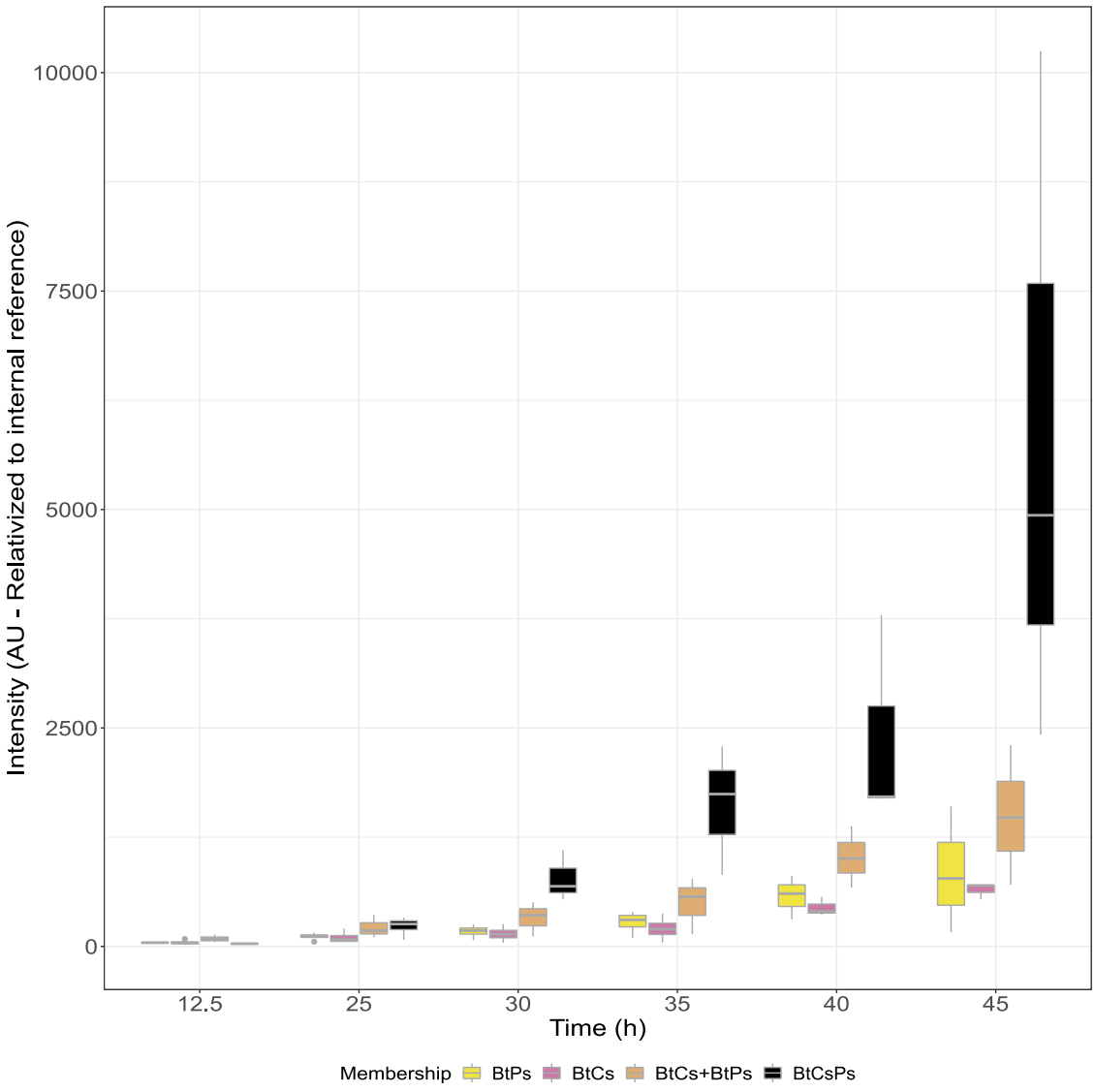
Intensity (AU - Relativized to internal reference)
10000
7500
5000
2500
0
12.5
25
30
35
40
45
Time (h)
Membership
BtPs
BtCs
BtCs+BtPs
BtCsPs

Table 1. Bacterial members used in the synthetic community (SynCom) system.

Member	***Burkholderia thailandensis E264***	***Chromobacterium subtsugae* ATCC 31532[a]**	***Pseudomonas syringae pv. tomato DC3000***
Genome size (Mb)	6.72	4.76	6.54
Family	*Burkholderiaceae*	*Neisseriaceae*	*Pseudomonadaceae*
No. of CDSs[b]	5 639	4 393	5 576
Chromosomes	2	1	1
Plasmids	0	0	2
ATCC	700388	31532	BAA-871
Reference	37	38	39

[a]This member in previous work [35, 36] was referred to as *Chromobacterium violaceum*. This member has been reclassified [40].

[b]CDSs, Coding sequences.